

THESIS FOR THE DEGREE OF DOCTOR OF PHILOSOPHY

**A mechanistic description of the evolution of aromatic tar during catalytic upgrading
of the raw gas produced from biomass steam gasification**

HUONG N. T. NGUYEN

Department of Space, Earth and Environment
CHALMERS UNIVERSITY OF TECHNOLOGY
Gothenburg, Sweden 2017

A mechanistic description of the evolution of aromatic tar during catalytic upgrading of the raw gas produced from biomass steam gasification

HUONG N. T. NGUYEN

ISBN 978-91-7597-665-5

© HUONG N. T. NGUYEN, 2017

Doktorsavhandlingar vid Chalmers tekniska högskola

Ny serie nr 4346

ISSN 0346-718X

Department of Space, Earth and Environment

Chalmers University of Technology

SE-412 96 Gothenburg

Sweden

Telephone + 46 (0) 31 772 1000

Printed by Chalmers Reproservice

Gothenburg, Sweden 2017

A mechanistic description of the evolution of aromatic tar during catalytic upgrading of the raw gas produced from biomass steam gasification

HUONG N. T. NGUYEN

Division of Energy Technology

Department of Space, Earth and Environment

Chalmers University of Technology

SE-412 96 Gothenburg, Sweden

Abstract

The removal of tar from the raw gas produced during biomass gasification is a prerequisite for the viability of the process downstream of the gasifier. The tar, the composition of which is dominated by aromatics, readily condenses, leading to process disruption. For upgrading the raw gas to remove the tar, the catalytic method enables the conversion of the tar into useful permanent gases at operating temperatures lower than that used in the alternative thermal method without catalysts. Understanding how the tar evolves during the raw gas upgrading process is essential for implementation of the catalytic method.

This work aims at improving the current understanding of the evolution of the tar during the raw gas upgrading. The focus is on capturing the principles of the product selectivity of the tar conversion with the presence of steam, H₂, and CO₂ in the raw gas as cracking and reforming agents, and on describing the main trends in the tar evolution. The catalytic method is the main focus, with the thermal method being investigated mainly for comparison. In terms of the main reaction pathways through which tar is converted, raw gas upgrading is a combination of different cracking and reforming processes used in petroleum refineries. Thus, the well-established knowledge of the relevant petrochemical processes is adopted as the basis for this work. Furthermore, to represent the real-life condition, raw gas that was produced in the Chalmers 2–4-MW_{th} dual fluidized bed biomass gasifier (an industrial-scale gasifier) was used in the experiments.

As the first step, a mechanism that explains the gradual conversion of tar and light hydrocarbons, as well as the main trends of product formation during the upgrading process was formulated. This mechanism was used to develop a kinetic model that provides a simplified description of the catalytic raw gas upgrading. The model takes into account eight groups of tar and light hydrocarbons that are present in the applied raw gas and that are indicative of the progress of tar evolution. The extents to which the parent tar/light hydrocarbons are converted into CO/CO₂ and into smaller tar/light hydrocarbons are taken as an input. The applicability of the model was demonstrated for the upgrading of the Chalmers raw gas in the presence of a

process-activated ilmenite catalyst that was obtained from the Chalmers 12-MW_{th} boiler. The evolutionary profiles of the tar and light hydrocarbon groups were derived. The results confirm that this model is able to capture the features of the upgrading process.

The tendency to produce polycyclic aromatic hydrocarbon (PAH) tar due to the mutual combination of carbon-containing intermediates, which is suggested in the mechanism, was investigated in relation to process severity in a steam and H₂-containing reaction environment. The results show that the growth of PAH tar can be suppressed, given that the process severity is sufficient to convert steam and H₂ into hydrogen intermediates, which prevents combination of the carbon-containing intermediates. The obtained results explain the fate of PAH tar during the late stage of tar maturation in steam gasification of biomass.

Overall, this work provides a generalized understanding of the evolution of tar during the raw gas upgrading. The similarity between raw gas upgrading and petrochemical processes is confirmed, which encourages further applications of the mature knowledge of the petroleum refinery to biomass gasification. Furthermore, the results provide essential inputs for the future development of more-comprehensive models, in that the complicated features of the upgrading process can be gradually resolved.

Keywords: biomass gasification, raw gas, tar, catalytic raw gas upgrading, kinetic model, ilmenite.

List of publications

This thesis is based on the following papers, which are referred to in the text by their Roman numerals:

- Paper I** Huong N. T. Nguyen, Nicolas Berguerand, Henrik Thunman. Mechanism and kinetic modeling of catalytic upgrading of a biomass-derived raw gas: An application with ilmenite as catalyst. *Industrial & Engineering Chemistry Research* 55, pp. 5843-5853, 2016.
- Paper II** Huong N. T. Nguyen, Nicolas Berguerand, Georg L. Schwebel, Henrik Thunman. Importance of decomposition reactions for catalytic conversion of tar and light hydrocarbons: An application with an ilmenite catalyst. *Industrial & Engineering Chemistry Research* 55, pp. 11900–11909, 2016.
- Paper III** Huong N. T. Nguyen, Nicolas Berguerand, Henrik Thunman. Applicability of a kinetic model for catalytic conversion of tar and light hydrocarbons using process-activated ilmenite. *Submitted for publication*.
- Paper IV** Huong N. T. Nguyen, Martin Seemann, Henrik Thunman. Fate of polycyclic aromatic hydrocarbons during tertiary tar formation in steam gasification of biomass. *Submitted for publication*

Author details

Huong N. T. Nguyen is the principal author of **Papers I–IV**. Dr. Georg L. Schwebel contributed to the experimental work, discussion, and editing of **Paper II**. Assistant Professor Nicolas Berguerand contributed to the experimental work, discussion, and editing of **Papers I–III**. Associate Professor Martin Seemann contributed to discussion and editing of **Paper IV**. Professor Henrik Thunman contributed ideas, discussion, and editorial support for all four papers.

Related publications not included in the thesis:

- A. Huong N. T. Nguyen, Nicolas Berguerand, Henrik Thunman. Process activated ilmenite as catalyst for cleaning of biomass producer gas. *4th International Symposium on Gasification and its Applications (iSGA-4), Vienna, Austria, 2014.*
- B. Huong N. T. Nguyen, Nicolas Berguerand, Henrik Thunman. Process activated ilmenite as catalyst for cleaning of biomass producer gas. *3rd International Conference on Chemical Looping, Gothenburg, Sweden, 2014.*

List of abbreviations

OC, oxygenated organic compounds

OLGA, oil-based gas washer (Dutch acronym)

CLR, chemical looping reforming

GC, gas chromatography

GC-FID, gas chromatography with a flame ionization detector

HC, light hydrocarbons

H/C, hydrogen-to-carbon ratio

PAH, polycyclic aromatic hydrocarbon

SNG, substitute natural gas

SPA, solid-phase absorption

WGS, water-gas shift (reaction)

Acknowledgement

Life holds adventures in every turn. To me, pursuing PhD is a great adventure. I am able to go that far thanks to supports from amazing people whom I have met along my journey.

First of all, I would like to express my sincere gratitude to my principal academic supervisor Henrik Thunman. Thank you for your enthusiasm, patience, and care that you have dedicated to raise me up in my scientific life. I would like to give my gratefulness to Nicolas Berguerand and Martin Seemann, my assistant academic supervisors. Thank you for interesting discussions and all helps along. To Fredrik Lind and Georg Schwebel, thank you for being my very first instructors training me in engineering experimental work. To Måns Collin, thank you for great ideas of petroleum refining you have brought to my research. On top of scientific lessons, I have learned from you the perspectives on life. To Vincent Collins, I appreciate very much for your thorough help to make my writings attractive.

I would like to thank Jessica Bohwalli, Johannes Öhlin, Rustan Hvitt and the operating staff at Chalmers Kraftcentral (KC). With your great help, I always feel “secured” in KC and I am certain that experiments are being successful.

I would like to thank all former and present colleagues in Gasification and Environmental Inorganic Chemistry groups. My special thanks go to Teresa, Mikael and Jelena for all helps with experiments and for fruitful discussions. You are like my “extra eye” with that I am able to perceive scientific challenges comprehensively. To all colleagues at the Division of Energy Technology, thank you for that you have created the best ever working environment. To Tove, my officemate, thank you for your support and for being always eager to explain my questions of all kinds, especially those about Sweden.

Thank you all my friends in ‘Ngu-ồn A1’ and in ‘Tài Năng 04’. You all have contributed to shaping my personality and making my life enjoyable, regardless of that years and years have passed. To Giang, Huyền and Chi, my special thanks go to you for being supporting by my side during the hard time.

Last but foremost, I would like to give my greatest gratefulness to my parents and my brother. Con cảm ơn Ba Mẹ, chị cảm ơn Tôm.

This work has been financially supported by E.ON and the Swedish Gasification Centre (SFC). Operation of the gasifier was supported by Göteborg Energi, Metso, Akademiska Hus, and the Swedish Energy Agency.

Huong Ngoc Thuy Nguyen
Gothenburg, November 2017

Table of contents

1. INTRODUCTION	1
1.1. Catalytic method: current research trends and limitations	3
1.2. Aim and methodology of the thesis	5
1.3. Outline of the thesis	7
2. THEORETICAL BACKGROUND	9
2.1. Tar formation and maturation during biomass gasification	9
2.2. Reactions and products of raw gas upgrading	10
2.3. Potential applications of petrochemical processes to raw gas upgrading.....	12
3. MECHANISM UNDERLYING THE CONVERSION OF TAR AND LIGHT HYDROCARBONS	15
3.1. Description of the mechanism	15
3.2. Applications of the mechanism	17
3.2.1. Towards smaller products.....	17
3.2.2. Towards larger products.....	18
4. A KINETIC MODEL FOR CATALYTIC RAW GAS UPGRADING	21
4.1. Description of the model.....	21
4.2. Empirical model coefficients representing product distribution	22
5. EXPERIMENTAL SECTION.....	25
5.1. Gasifier operation and raw gas properties.....	25
5.1.1. Gasifier operation	25
5.1.2. Raw gas properties	26
5.2. Gas upgrading experiments.....	27
5.2.1. Activation of ilmenite.....	27
5.2.2. Experimental setups	28
6. RESULTS AND DISCUSSION.....	31
6.1. Contribution of decomposition reactions to the conversion of tar and light hydrocarbons .	31
6.2. Evaluation of the kinetic model.....	33
6.2.1. Composition of upgraded gas.....	33
6.2.2. Activation energy of tar and light hydrocarbons.....	39
6.3. Fate of PAH tar during the tertiary conversion of steam gasification of biomass	41

6.3.1.	Contributions of thermal and catalytic effects to process severity.....	41
6.3.2.	Growth of PAH tar.....	43
6.4.	General discussion and suggestions for future studies.....	46
6.4.1.	General discussion	46
6.4.2.	Suggestion for future studies.....	48
7.	CONCLUSIONS AND OUTLOOK.....	49
	REFERENCES.....	51

1. Introduction

Biomass gasification, which is a thermochemical process in that biomass is converted into an energy-rich raw gas, represents an attractive technology for reducing CO₂ emissions and our current dependence on fossil fuels [1-3]. In this process, air, oxygen, steam or mixtures thereof are added as gasifying agents. Heat is supplied through either the direct combustion of part of the input biomass or by some other means, for example, the circulation of hot bed materials. The gasification yields a raw gas that consists mainly of: steam; permanent gases H₂, CO, CO₂, and methane (CH₄), and other light hydrocarbons (HC), such as ethene (C₂H₄); and condensable organic compounds, known as 'tar' [1-3]. The produced raw gas can be burned directly to produce heat, integrated with gas turbines or fuel cells to produce electricity, or used to synthesize high-grade products, such as substitute natural gas (SNG), methanol, Fischer-Tropsch fuels, and other chemicals [3, 4]. Except when the raw gas is used for heat production, prior to other envisaged uses, the tar in the raw gas must be removed. Indeed, tar can already condense at about 350°C, which can cause blockages of downstream items of equipment and, subsequently, process disruption. Furthermore, the chemical energy of the tar can account for up to 15% of the energy content of the dry and ash-free biomass feedstock. Thus, tar removal is essential to maintain the viability of the process downstream of the gasifier, and it can contribute to improving the cold gas efficiency of the gasification process if the chemical energy stored in the tar is recovered [5-8].

Considerable efforts have been dedicated to reducing the tar content of the raw gas. A gasifier of given design regarding the gasification process, biomass feedstock, and gasifying agents can be operated at the highest possible temperature and gas residence time so as to minimize the tar yield [1, 5, 9]. As a consequence, the composition of the tar in the produced raw gas is dominated by aromatics [7, 9, 10]. Particularly in the case of fluidized bed gasifiers, an alternative strategy to reduce the tar yield is to use catalytic materials as the bed inventory instead of inert silica sand [9, 11-13]. These methods of tar abatement implemented inside the gasifier are known as primary measures. They are utilized to mitigate the effort required for tar removal measures implemented downstream of the gasifier, which are known as secondary measures. If the envisaged use of the raw gas is to synthesize high-grade products, in which the catalysts used for these syntheses are easily deactivated by the contaminants, the tar in the raw gas must be at a very low level (e.g., <1 mg/Nm³ for methanol and Fischer-Tropsch syntheses [3, 8]; this value corresponds to about 0.3 ppm assuming that tar contains exclusively benzene). In this situation, the use of secondary measures is particularly crucial, regardless of the primary measures employed.

Table 1. Main approaches to secondary measures for tar removal.

Physical approach	Chemical approach	
<ul style="list-style-type: none"> - Wet scrubbing - Electrostatic precipitation 	<ul style="list-style-type: none"> - Using catalysts (600–900°C) 	<ul style="list-style-type: none"> - Without using catalysts (≥1100°C)
<ul style="list-style-type: none"> - Adsorption - Cyclone separation 	<p>Heat supply to the process:</p> <ul style="list-style-type: none"> - Direct heat supply: injecting air/pure O₂ stream or using oxygen from oxygen carriers to combust part of the raw gas - Indirect heat supply: for example, circulating hot bed material 	

The secondary measures for tar removal can be classified as physical or chemical approaches, as summarized in Table 1. In the physical approach, the tar is physically removed from the raw gas. Typical methods for achieving this are listed in the table. Of these, the wet scrubbing method is widely employed owing to its competitive efficiency and investment cost, as compared to other physical means. In this method, water or organic scrubbing media are used to absorb the tar. Using water, the tar removal efficiency is low due to the hydrophobicity of the tar, and wastewater treatment is compulsory before the water can be discharged. Using organic scrubbing media, a higher removal efficiency, especially for non-polar tar components, is achieved. However, the significant costs linked to purchasing the fresh media and recycling the spent media represent a challenge. In addition, the wet scrubbing method potentially entails a thermal penalty. This problem is related to the high levels of gas cooling and reheating required for the subsequent gas conditioning or syntheses, e.g., gas cooling from temperatures in the range of 800–900°C at the outlet of a dual fluidized bed gasifier to about 60–80°C at the outlet of an OLGA unit (an oil-based gas washer for tar removal), and gas reheating to 200–350°C required for SNG synthesis [14-21].

In the chemical approach, the tar is chemically converted into useful permanent gases, such as CH₄, CO, and H₂, which can contribute to increasing the cold gas efficiency of the gasification. The conversion of tar takes place most likely *via* decomposition reactions, i.e., thermal cracking, hydro-cracking, steam reforming, and dry reforming, which resemble the principal reaction pathways of petrochemical processes [22-31]. To sustain the endothermic tar conversion, heat can be supplied either directly by combusting part of the inlet raw gas or indirectly by, for example, circulating the hot bed material if the tar conversion is conducted in a dual fluidized bed reactor. In the direct heat supply system, either an air/O₂ stream is injected into the raw gas or oxygen can be provided *via* oxygen carriers; soot formation and increases in the level of CO₂ in the gas obtained after the tar treatment can be problematic. These problems, however, do not apply to the indirect heat supply [32-35]. The tar can be converted in the presence of catalysts

(hereinafter termed the ‘catalytic method’) or without using catalysts (hereinafter termed the ‘thermal method’). For the catalytic method, an operating temperature in the range of 600–900°C is efficient; this temperature range promotes the thermal integration of the tar removal unit with the outlet of the fluidized bed gasifier [1, 20, 36-39]. For the thermal method, an operating temperature of at least 1100°C is required [6, 19, 33]. Thus, the catalytic method is more beneficial in terms of the heat demand. The catalytic method is the main focus throughout this thesis; for comparison, the thermal effects under relevant conditions are also investigated.

1.1. Catalytic method: current research trends and limitations

Current research on the catalytic method for secondary tar removal follows two main trends: (i) screening potential catalysts and integrating the catalysts into the process downstream of the gasifier; and (ii) gaining an understanding of the evolution of tar, especially of aromatic species, which occurs during tar removal.

The first trend (i) has attracted the most attention. The aim here is to identify catalysts that are: efficient in terms of catalytic activity; resistant to attrition; resistant to deactivation by carbon deposits, sulfur, and chloride or that are easily regenerated from these contaminants; available at an acceptable price; and environmentally friendly. Various synthetic and naturally occurring catalysts have been investigated. Based on the chemical composition, the catalysts can be classified into alkali metal-, alkaline earth metal-, transition metal-, and zeolite-based catalysts, and char [8, 18, 39, 40]. Nickel-based catalysts, which are widely used for naphtha reforming and methane reforming in the petrochemical industry, have been proven to be among the most effective catalysts for tar removal [6, 39, 41]. However, nickel is toxic and represents an environmental hazard. Therefore, naturally occurring and inexpensive materials, such as olivine, limonite, ilmenite, and dolomite, are attracting interest, despite their low catalytic activities compared to nickel catalysts [13, 14, 40, 42].

In addition to the effort being put into screening potential catalysts, there is an ongoing search for ways to integrate the catalysts into the process downstream of the gasifier, to achieve the required level of tar removal efficiency, while reducing the capital and/or operating costs. An example of this is the development of the chemical looping reforming (CLR) system for combining continuous tar removal with simultaneous catalyst regeneration, e.g., from carbon deposited on the catalyst surface, as has previously been proposed by the same research group as that in the present work [35, 43, 44]. The CLR system is configured as a dual fluidized bed unit, in which tar is converted in one reactor and the used catalyst is simultaneously regenerated in the other reactor. Through simultaneous regeneration, the deactivation of catalyst is mitigated, such that the frequency of catalyst renewal is reduced. Furthermore, heat released from the combustion of carbon deposits can contribute to the heat demand required for the tar conversion. The CLR concept can be applied directly to dual fluidized bed gasifiers, whereby the number of downstream reactors intended for tar removal is reduced. This is accomplished by

utilizing the fine fraction of the catalytic material used as the bed in the gasifier. In the gasification chamber, the coarse particles remain in the dense bed, provide mixing and acting as the heat carrier, while the fine particles act as a catalyst in the freeboard. As the fine particles exit the gasification chamber, they are collected and injected into the combustion chamber for regeneration; as they leave the combustion chamber, they are collected to be transferred back into the gasification chamber [45].

To derive an efficient catalytic method, as well as a thermal method to reduce or eliminate the tar, understanding the evolution of tar during its removal is essential. However, the number of research studies focused on gaining this understanding, i.e., the second trend (ii), is limited. The main difficulty lies in the inherently complex composition of the tar, i.e., hundreds of tar species are present in the raw gas, and in the numerous reactions occur during tar removal [6, 7]. In the literature, elucidating the mechanism and kinetic parameters of the conversion of single tar components and formulating kinetic models that describe the tar removal process are the two main topics [4, 7]. In many studies, aromatic tar components that are present at significant levels in the raw gas, such as benzene, toluene, and naphthalene, are investigated individually [46-51]. However, this approach of investigating single tar components cannot by itself mirror the authentic tar removal process, since the tar mixture in the raw gas contains numerous components, as mentioned earlier.

As the formulation of kinetic models is a more complex task, fewer studies have been performed. First, the models are required to be able to describe comprehensively the principal routes of evolution of the tar during the removal process. Second, the models should be able to predict the process, which provides inputs for the optimization and upscaling. To fulfill these two requirements, an appropriate description of the model and a sufficient input of experimental data are necessary. To resolve the difficulty associated with the complexity of the tar composition, two main approaches have been investigated. The first approach is to take into account the entire tar mixture of the raw gas and divide it into different groups based on reactivity, which is the case for the lump models [52-54]. The second approach is to include in the models only the individual and representative aromatic tar components. Several authors have incorporated this type of model into the modeling of the gasification process as a whole, i.e., secondary tar removal is treated as the conversion of the gas product produced from the pyrolysis of biomass feedstock [32, 55-57]. The tar components inputted to the model represent different stages during the progression of the gasification/secondary tar removal, and they are selected based on experimental observations.

In the lump models, as well as in the models based on representative tar components, a certain number of conversion pathways between the tar groups or between the representative tar components are incorporated. The kinetic parameters of the incorporated conversion pathways are taken from different experimental studies available in the literature, or they are derived by fitting the developed model to the experimental data. In this way, the models can

describe the processes that have similar characteristics as those of the conducted investigations in which the models were developed. Furthermore, whether or not the models represent the authentic processes is dependent upon the reliability of the inputted experimental data. Thus, the models referred to in the literature as ‘detailed kinetic models’, which do not attempt to simplify the complexity of the tar removal process, are more comprehensive than the other models discussed above, and they are also developed [58, 59]. In the detailed kinetic models, hundreds to thousands of elementary reactions are included, thereby incorporating into the models all the reaction pathways and products that are theoretically possible. Thus, unless sufficient experimental observations are provided as guidance to select the elementary reactions, these models will represent tools with a lack of practical applications.

1.2. Aim and methodology of the thesis

Given the current gaps in our understanding of the evolution of tar during the secondary removal process, this work is motivated. The aim of this thesis is to capture the principles of the product selectivity of the tar conversion, and to describe the principal trends in the evolution of the tar during removal. In this way, the obtained results are to be applied to general processes and to be used as inputs for the improvement of the available detailed kinetic models. It should be emphasized that the well-established knowledge in the petroleum refinery is taken as the basis for this work, since the reaction pathways for tar conversion are similar to the petrochemical processes, as mentioned earlier.

To accomplish this aim, several steps are carried out (visualized in Figure 1); the details are presented in the four papers attached to this thesis, i.e., **Papers I–IV**. In the first step, a mechanism is formulated, which explains the gradual conversion of tar and light HC, as well as the main trends of product formation. This mechanism simplifies the upgrading process into interactions between three different types of reactive intermediates, i.e., carbon-containing intermediates (C^*), hydrogen intermediates (H^*), and oxygen intermediates (O^*), in which C^* originate from tar and light HC, and H^* and O^* originate most likely from a steam, H_2 , and CO_2 mixture that is available in the raw gas. Depending on the interaction that occurs, different types of products can be observed, including oxidation products (i.e., CO/CO_2), tar/light HC smaller than the parent tar/light HC, and tar/light HC larger than the parent tar/light HC. Based on the mechanism, a kinetic model that describes the catalytic upgrading of a raw gas is developed. The model takes into account eight groups of tar and light HC that are present in the applied raw gas and that are indicative of the progress of tar evolution. The model requires an input that reflects the extent to which the parent tar/light HC is converted into CO/CO_2 and into smaller tar/light HC. In this respect, knowledge about the contributions of the different decomposition reactions to the conversion of tar and light HC is required. The model is further used with experimental data to derive the evolutionary profiles of the tar and light HC groups. Finally, the mechanism for producing larger products is applied to elucidate the formation of polycyclic aromatic

hydrocarbon (PAH) tar from the PAH precursor, which takes place during the late stage of tar maturation during biomass gasification. It should be noted that hereinafter, the term ‘raw gas upgrading’ will be used instead of ‘secondary tar removal’. Indeed, during the tar removal process, in addition to the conversion of tar, reactions involving the permanent gases, such as the water-gas shift (WGS) reaction and the conversion of light HC, also take place.

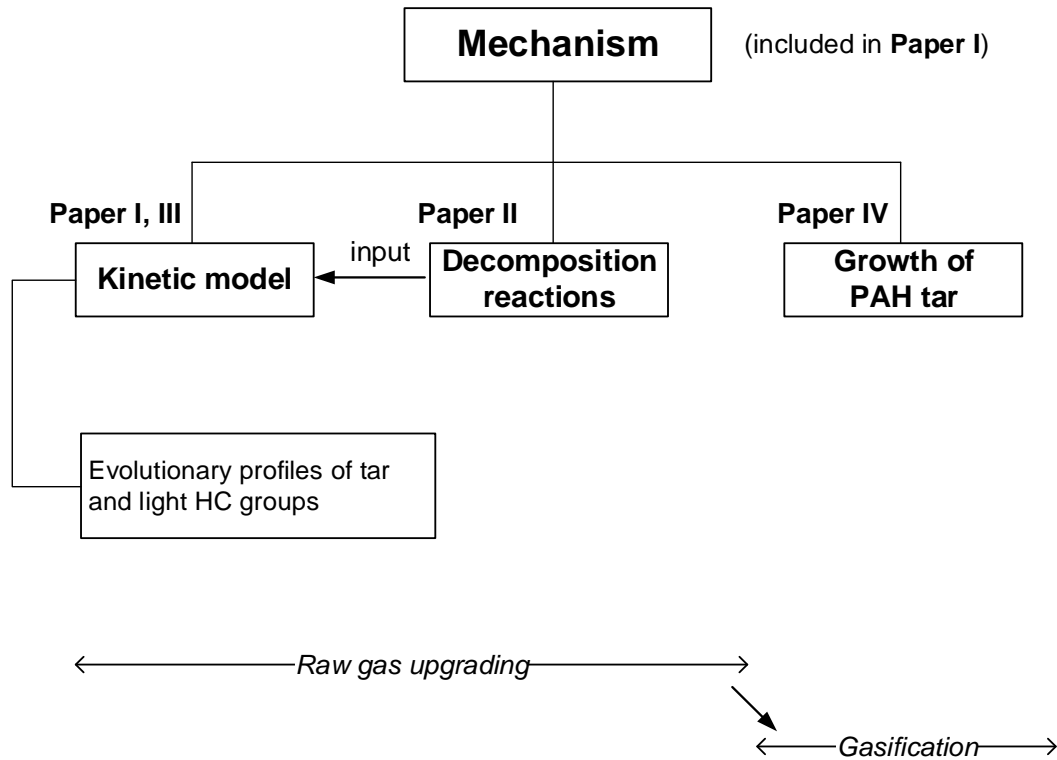


Figure 1. Steps towards the accomplishment of the aim of this thesis.

The choices of raw gas and catalyst for conducting the required experiments are based on the following criteria:

Choice of raw gas

A mature tar-containing raw gas, which is produced in the Chalmers 2–4-MW dual fluidized bed biomass gasifier (hereinafter abbreviated as the Chalmers raw gas and Chalmers gasifier, respectively) operated at 820°C and a gas residence time of about 5 s, is used for the following reasons:

- The raw gas is produced from an industrial-scale gasifier. Aromatics represent the major composition of the tar in the raw gas; the aromatics range from benzene to coronene in terms of boiling temperature. The investigations using this raw gas, therefore, represent authentic processes. Specifically, the entire aromatic-tar spectrum involved in the gasification is considered.

- CH₄ and other light HC, such as C₂H₄, are present in significant amounts, the conversion of which can be incorporated into the progression of tar evolution. Indeed, the conversion of tar can produce light HC, and the conversion of the light HC may make an important contribution to the final composition of the upgraded gas; and
- Steam is used as the gasifying agent, and the WGS reaction takes place to a significant extent during the gasification. Thus, the produced raw gas contains significant levels of steam, H₂, and CO₂, i.e., about 60 vol%, 8 vol%, and 5 vol% on a wet basis, respectively. The use of this raw gas facilitates elucidation of the roles of these agents in the conversion of tar and light HC.

Using ilmenite as the catalyst

Ilmenite, which is an iron titanium oxide with chemical formula of FeTiO₃, is used as a catalyst. Ilmenite is selected based on the following features:

- Ilmenite is known to facilitate the destruction of heteroatom-containing and branched tar components, as well as light HC, such as C₂H₄. However, it is not sufficiently active to convert CH₄ and non-branched aromatic tars, such as benzene and naphthalene [35, 43, 60]. With this moderate catalytic activity of ilmenite, a gradual evolution of tar and light HC in relation to the contact time between raw gas and solid catalyst (abbreviated as the ‘gas-solid contact time’) can be expected. Furthermore, carbon deposition on ilmenite particles during the upgrading process in an environment of excess steam is negligible, which mitigates the complexity of the reaction network [35, 43, 61]; and
- Ilmenite is naturally occurring, inexpensive compared to synthetic materials, and attrition-resistant, all of which promote ilmenite as a potential catalyst for commercial applications, especially in fluidized bed systems.

1.3. Outline of the thesis

The thesis is organized as follows. After this Introduction (Chapter 1), Chapter 2 presents the theoretical background relevant to this work. The theories about tar formation and maturation during biomass gasification, the main reactions and products observed for the raw gas upgrading, and the potential applications of petrochemical processes to raw gas upgrading are summarized. In Chapter 3, the developed mechanism that underlies the conversion of tar and light HC during raw gas upgrading, and applications of the mechanism are presented. Chapter 4 describes the kinetic model for catalytic raw gas upgrading. Chapter 5 is the experimental section, in which the operating conditions of the Chalmers gasifier and the composition of its raw gas, as well as the experiments performed for the gas upgrading are outlined. Chapter 6 discusses the main results. In particular, the results of the contributions of decomposition reactions to the conversion of tar and light HC, the evaluation of the kinetic model, and the fate

of PAH tar in the tertiary conversion stage of biomass steam gasification are presented. In Chapter 6, suggestion for future studies is also discussed. Finally, the main conclusions of the work and outlook are outlined in Chapter 7.

2. Theoretical background

2.1. Tar formation and maturation during biomass gasification

The gasification process with the focus on the maturation of tar is described in Figure 2, which summarizes the literature describing the different aspects of biomass gasification [5, 6, 10, 56, 62-69], as well as the literature that deals with the increases in molecular size of aromatic compounds [70-77]. It is worth noting that in the literature on biomass gasification, the criteria to classify tar compounds according to the degree of maturation, and the classification of the conversion stages that occur in the gasification process are not consistent [6, 78]. In this thesis, the definitions of 'primary tar', 'secondary tar', and 'tertiary tar' follow the definitions proposed by Evans and Milne [10, 62]. The 'primary conversion', 'secondary conversion', and 'tertiary conversion' stages presented in Figure 2 are named after the type of tar produced, which should be viewed in relation to the evolution of tar itself, rather than in relation to the conversion of biomass as a whole. Indeed, cellulose, hemicellulose, and lignin, which constitute the biomass, differ in chemical structure and reactivity, which means that they are converted differently during the gasification process. Finally, the extractives in the biomass are not considered here due to their low content in woody biomass [3, 79], which is the fuel used in this work.

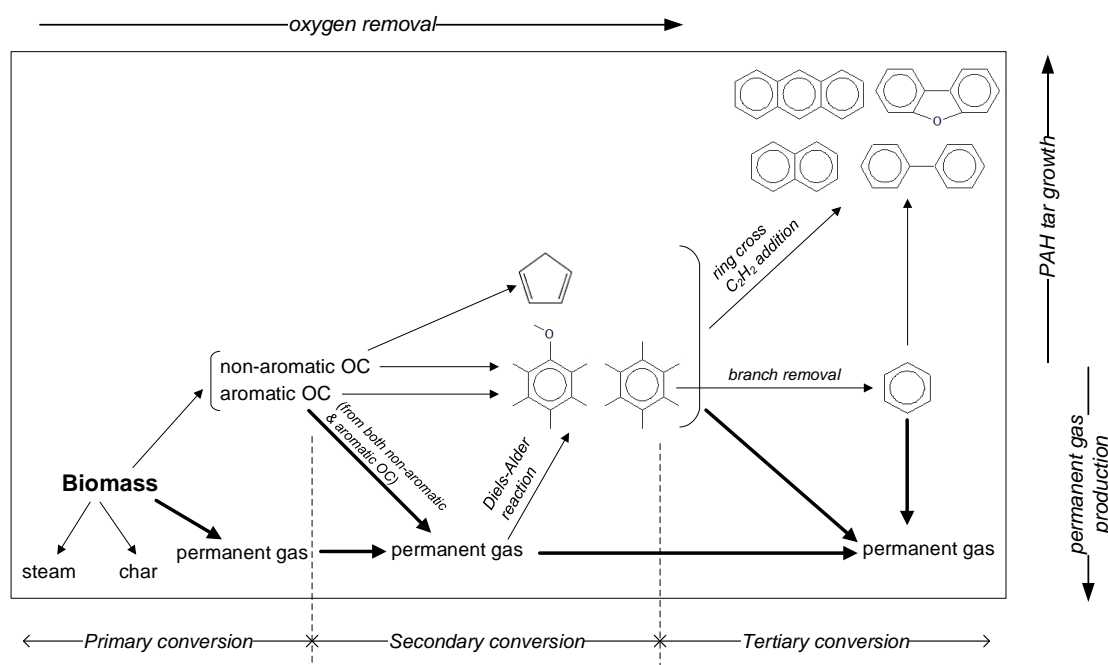


Figure 2. Biomass gasification with the focus on the maturation of tar. OC denotes oxygenated organic compounds. Reaction pathways that produce permanent gases are represented by thicker arrows, to indicate that they are the main routes throughout the gasification process. Reactions of char are not included.

Depending on, for example, the operating temperature of the gasifier and the residence time of the raw gas, in general, the tar evolves from oxygenated organic compounds (OC) during primary conversion to PAH precursors during secondary conversion, and finally to PAH tar in the tertiary conversion (Figure 2). Furthermore, the tar becomes more thermally stable, oxygen is gradually removed from the tar, and eventually the tertiary tar contains a negligible amount of oxygen. The OC have chemical compositions similar to that of the feedstock biomass, and consist of non-aromatic compounds derived mainly from cellulose and hemicellulose and aromatic compounds derived mainly from lignin. The PAH precursors are either non-aromatic compounds, such as cyclopentadiene, or monocyclic aromatics. The non-aromatic precursors are most likely produced from the non-aromatic OC. The monocyclic aromatic precursors are produced from both non-aromatic and aromatic OC, i.e., non-aromatic OC are transformed into monocyclic aromatics, and aromatic OC are converted to become less-branched and less-oxygenated [62, 64]. The monocyclic aromatic precursors are also produced *via*, e.g., the Diels-Alder reactions of light alkenes, such as ethene, propene, and butene in the permanent gas, followed by dehydrogenations of the formed cyclic hydrocarbons [62, 70].

After the PAH precursors are formed, two main pathways can be followed: towards the formation of smaller products, such as permanent gases; and towards the formation of larger products, i.e., PAH tar. The extent to which these pathways take place depends on the reaction environment in the gasifier, as well as on the operating conditions, such as temperature. The growth of PAH tar occurs mainly *via* two main mechanisms: (i) ring cross, e.g., combination of two aromatic species; and (ii) consecutive additions of unsaturated light hydrocarbons [such as ethyne (C_2H_2)] that are produced during the tertiary conversion stage, to an aromatic intermediate, which is followed by cyclization and dehydrogenation, and ultimately results in an increase of the number of aromatic rings in the PAH tar molecules [69-77]. It is noteworthy that the reaction of non-aromatic precursors creates aromatics, e.g., the reactions of two cyclopentadiene molecules result in one naphthalene molecule, which can further mature into heavier PAH tar *via* the two above-mentioned mechanisms [70, 74].

2.2. Reactions and products of raw gas upgrading

The most important reactions associated with the upgrading process, reported in the literature, are summarized in Table 2 [8, 35, 41, 80-82].

Table 2. The most important reactions in raw gas upgrading.

Reaction	Formula
Thermal cracking	$C_xH_y \rightarrow C_{x'}H_{y'} + C + H_2$ (R1)
Hydro-cracking	$C_xH_y + H_2 \rightarrow C_{x'}H_{y'}$ (R2)
Steam reforming	<ul style="list-style-type: none"> • Steam dealkylation $C_xH_y + H_2O \rightarrow C_{x'}H_{y'} + CO + H_2$ (R3) <ul style="list-style-type: none"> • Complete steam reforming $C_xH_y + H_2O \rightarrow CO + H_2$
Dry reforming	$C_xH_y + CO_2 \rightarrow CO + H_2$ (R4)
WGS	$CO + H_2O \rightleftharpoons CO_2 + H_2$ (R5)

The decomposition reactions through which tar and light HC are converted include thermal cracking, hydro-cracking, steam reforming, and dry reforming, i.e., R1–R4, respectively. The steam reforming reaction is either steam dealkylation, during which other tars and light HC ($C_{x'}H_{y'}$) are produced, or complete steam reforming, which generates only CO and H_2 . The formation of carbon deposits is included in the thermal cracking reaction. In addition to the decomposition reactions, the WGS reaction may occur. To aggregate the reactions presented in Table 2 and to describe in general the upgrading process in terms of the reactions taking place and products formed, a simplified reaction scheme is proposed in Figure 3.

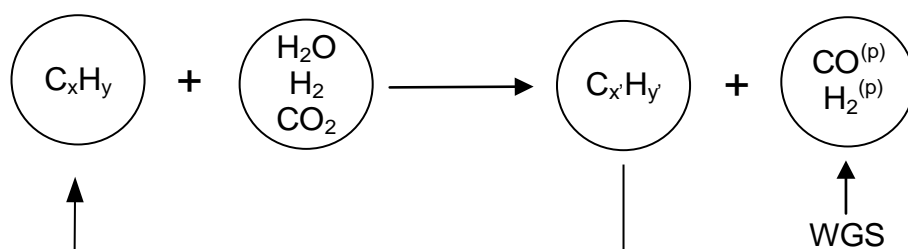


Figure 3. Simplified reaction scheme for raw gas upgrading. $CO^{(p)}$ and $H_2^{(p)}$ represent CO and H_2 as products, respectively.

In a reaction environment with surplus steam, i.e., the reaction environment relevant to the present work, carbon deposition is often negligible [61]. The oxidation product of CO/ CO_2 and the tar/light HC that are smaller and more stable than the parent tar/light HC in the raw gas are the two main types of carbon-containing products, as shown in Figure 3. Indeed, in addition to CO and CO_2 , it has been reported in the literature that tar and light HC can be produced. For example, CH_4 , which is the most stable light HC due to the sp^3 hybridization in its molecular structure, has been shown to be produced at significant levels when the ilmenite catalyst was

used at 800°C for raw gas upgrading. Furthermore, benzene and naphthalene, which are among the most stable tar components, were observed to be increased considerably in the upgraded gas [35, 43]. This was attributed to the fact that phenols, 1-ring aromatic and 2-ring aromatic compounds present in the used raw gas were readily stripped of their hydroxy and alkyl groups to form non-branched benzene and naphthalene. Tar molecules are primarily fragmented at the chemical bonds that have lower bond-dissociation energies, such as the carbon-hetero atom bond of C-O and the C-C bonds between the aromatic rings and the side-chains. The aromatic rings without branches are the most difficult to break owing to their aromaticity [64, 78, 83-88]. In addition to the CO/CO₂ and smaller tar/light HC that are produced from the above-discussed decomposition reactions, tar molecules larger than those in the raw gas have also been detected as side-products of the upgrading [47, 80, 89].

2.3. Potential applications of petrochemical processes to raw gas upgrading

With the exception of the dry reforming reaction, the decomposition reactions presented in Table 2 are the main reaction pathways of the different petrochemical processes. Therefore, the idea is to use the principal chemistry of these processes to explain the raw gas upgrading. Figure 4 summarizes the main features of the relevant petrochemical processes. In general, following the direction of the arrow in the figure, the processes reduce the molecular size and increase the hydrogen-to-carbon molar ratio (abbreviated as 'H/C ratio') of the products, as compared to the crude oil feedstock. The processes are divided into three categories, which differ in terms of the extents to which the cracking and reforming agents, i.e., steam and H₂, participate in the processes.

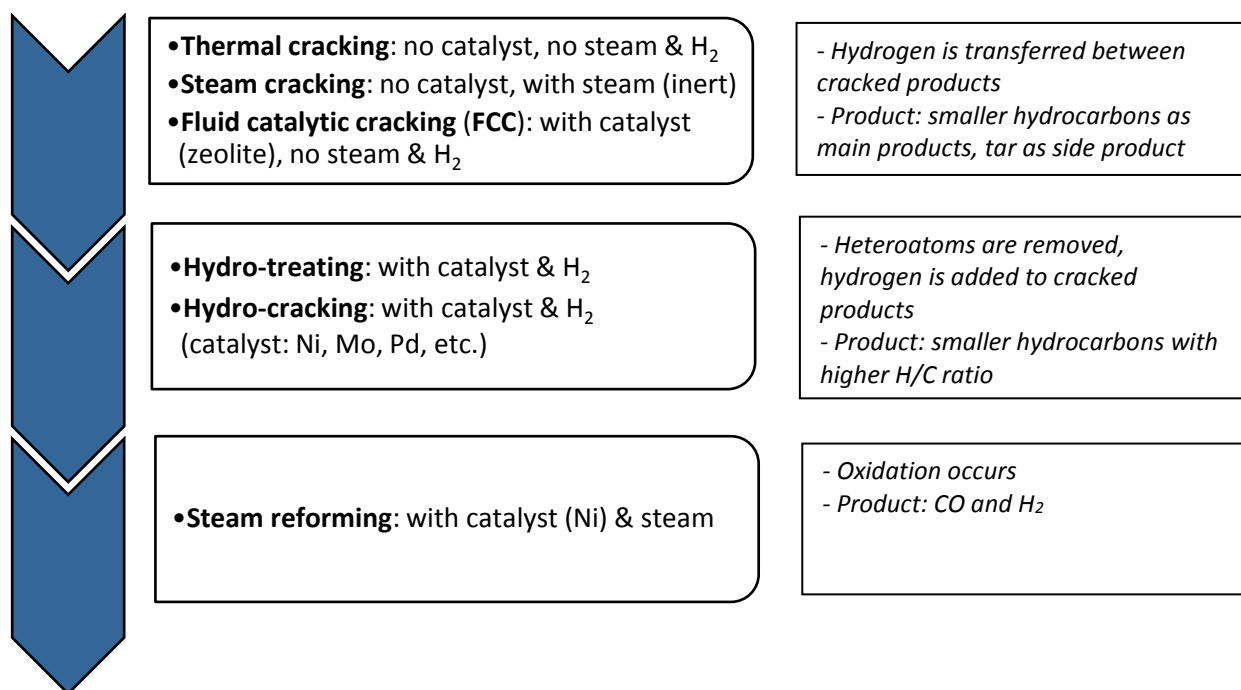


Figure 4. Petrochemical processes relevant to raw gas upgrading.

For thermal cracking, steam cracking, and fluid catalytic cracking (FCC), steam and H₂ are not used, or steam is added to dilute the concentration of the feedstock. In these processes, hydrogen is transferred between the cracked products. Smaller HC are produced as the main products. In addition, products that are heavier than the feedstock, such as tar, can also be formed [25-27, 90]. Hydro-treating and hydro-cracking are conducted mainly to remove sulfur, nitrogen, and oxygen, and to produce gasoline and diesel from relatively higher molecular weight feedstocks, respectively. H₂ is added to these processes as a reactant for the reactions. Therefore, the H/C ratio of the products is higher than that of the feedstock. Theoretically, in the hydro-cracking process, the H/C ratio can be increased from that of the crude oil (i.e., about 1.4–2.0) up to 4.0 if CH₄ is the final product [24, 28]. It is worth noting that in practice, the production of CH₄ requires relatively severe conditions and it is not usually expected as a product [24]. Furthermore, the presence of H₂ in the hydro-cracking process is known to reduce tar formation, as compared to, for example, the thermal cracking discussed above [22, 24, 25, 29, 30]. Due to the reactions between hydrogen intermediates and carbon-containing intermediates, the potential for the carbon-containing intermediates to combine mutually to produce heavier products is reduced [22].

In the steam reforming process, steam is used as an oxidation agent, and feedstocks, such as CH₄ and low-boiling-point naphtha, are converted into CO and H₂ [23, 31]. From the discussed processes, it can be noticed that when steam or H₂ is participating as a reactant in the conversion of the feedstocks, a catalyst is required. As an example, steam cracking and steam reforming are conducted at similar temperatures and residence times (i.e., temperatures in the range of 700–

900°C and residence times of several milliseconds to about 2 seconds). However, a nickel catalyst is used in steam reforming, so that oxidation by steam can occur [23, 27, 31, 90].

Overall, several features of the petrochemical processes can be adopted to explain raw gas upgrading process. These features are: cracking into relatively smaller products as the main pathway; forming heavier products through the combination of carbon-containing fragments as the side pathway; increasing the H/C ratio of the products by the addition of hydrogen atoms; and oxidizing carbon fragments to CO using the oxygen from steam. Each of the categories of the petrochemical processes are distinguished regarding the nature of the products formed, which is mainly attributed to the participation of steam and H₂ in the processes. Even when these different processes (i.e., different decomposition reactions in the context of the raw gas upgrading) occur simultaneously, their individual contributions can be identified based on the nature of the products obtained. In this way, the strategy of generalizing the numerous reactants taking part in the upgrading process into representative reactive species that directly determine the nature of the product can facilitate the description of the upgrading process in more general terms.

3. Mechanism underlying the conversion of tar and light hydrocarbons

In this chapter, the mechanism based on reactive intermediates, which describes the gradual conversion of tar and light HC during raw gas upgrading is proposed. This reactive intermediate-based mechanism is largely based on the free radical mechanism that is well-described for the homogenous thermal cracking [78, 83, 90]. The free radical mechanism has also been applied to the heterogeneous catalytic decomposition of dedicated tar components in the gasification context [50, 91]. In the present work, a more general term ‘reactive intermediate’ is preferred over ‘free radical’, as reactive species other than free radicals can be formed on the catalyst surface when a solid catalyst is used. The features of the petrochemical processes discussed earlier are incorporated into the proposed mechanism. Furthermore, the assumptions made in the mechanism are mainly based on several studies [37, 50, 51, 78, 82, 92-98].

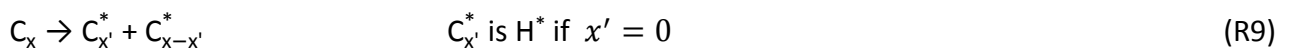
3.1. Description of the mechanism

The tar and light HC molecules are assumed to be initially converted into reactive intermediates, and it is only in this form that they can react further. To take into account the role of steam, H₂, and CO₂ in the conversion of tar and light HC, these cracking and reforming agents are also assumed to be converted into reactive intermediates. More precisely, steam, H₂, and CO₂ are converted into hydrogen intermediates H* and oxygen-containing intermediates O* following reactions R6–R8:

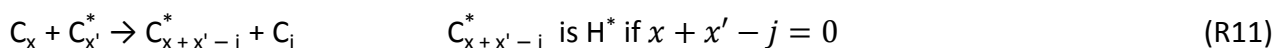


The gradual conversion of tar and light HC is described as follows *via* elementary reactions R9–R16. In these reactions, the symbols C with subscripts indicate tar and light HC molecules, the symbols C* with subscripts indicate carbon-containing reactive intermediates, and the subscript letters represent the number of carbons in the molecules or reactive intermediates.

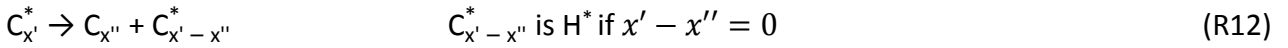
- Self-dissociation of tar and light HC molecules:



- Interaction between tar/light HC molecules and reactive intermediates:



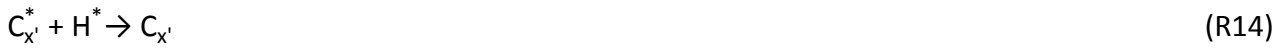
- Decomposition of tar and light HC intermediates:



- Addition of unsaturated HC to reactive intermediates:



- Termination:



- Oxidation :



Elementary reactions R9–R11 represent the main steps through which the tar and light HC reactive intermediates are initially generated, which include: self-dissociation of the tar and light HC molecules; interactions between tar/light HC molecules and H^* ; and interactions between tar/light HC molecules and tar/light HC reactive intermediates. R9–R11 are assumed to be the rate-determining steps during the conversion of tar and light HC. After formation, the tar and HC reactive intermediates can be decomposed to smaller species (R12) or to react with unsaturated HC, such as C_2H_2 , to form larger intermediates (R13). In the termination step, the tar and light HC intermediates react either with H^* [to produce relatively lighter products (R14)] or with other tar and light HC intermediates [to produce relatively heavier products (R15)]. It is assumed that once the reactive intermediates that contain only one carbon atom C_1^* are produced, e.g., after gradual fragmentation *via* R12, they can react with oxygen-containing intermediates O^* , to produce CO, and thereafter, to produce CO_2 *via* the WGS reaction.

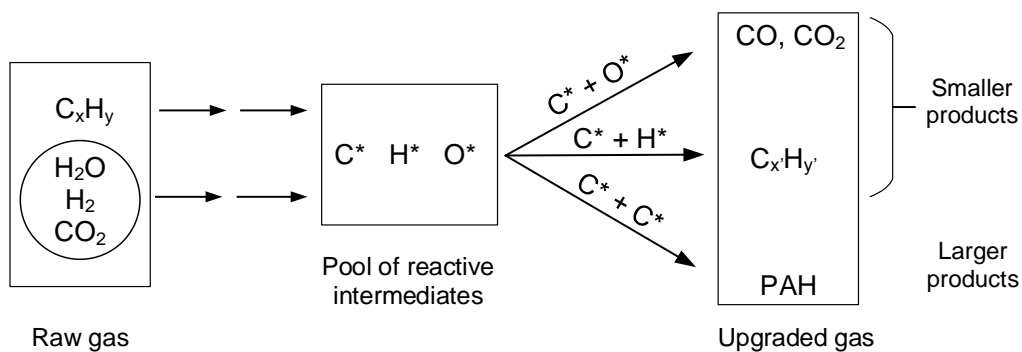


Figure 5. Summary of the proposed mechanism with the focus on product selectivity.

Overall, the proposed mechanism describes the gradual conversion of tar and light HC, as well as the main trends of product formation. The roles of steam, H_2 , and CO_2 are incorporated into the mechanism, i.e., H^* facilitate the initial conversion of tar and light HC molecules into C^* , and

H^* and O^* determine the nature of the products formed. Figure 5 summarizes the mechanism with the focus on product selectivity. By assuming that all the reactants in the raw gas must be converted into reactive intermediates to be able to react further, the reaction environment of the raw gas upgrading can be regarded as a pool that contains three types of reactive intermediates, C^* , H^* , and O^* . The nature of the products formed during the upgrading process depends on whether C^* react with O^* or with H^* , or whether C^* react with themselves. Thus, the nature of the product relates directly to the concentrations of the reactive intermediates in the pool.

For a given raw gas composition, the level of operating conditions used for the upgrading process, which in the present work is referred to as 'process severity', is the major factor determining the concentrations of the reactive intermediates. Process severity reflects three operating conditions of the reactor in which the raw gas upgrading is conducted: the temperature; the gas residence time in the reactor; and the gas-solid contact time when catalysts are present. In this way, the process severity includes the thermal effect and catalytic effect. In general, increasing the temperature and gas residence time enhances the thermal effect, whereas increasing the temperature and gas-solid contact time enhances the catalytic effect. Furthermore, the strength of the catalytic effect depends on the catalytic activities of the catalysts used.

3.2. Applications of the mechanism

3.2.1. Towards smaller products

In terms of the formation of lighter products, Figure 5 shows, in a simplified way, the aggregate effects of the decomposition reactions presented in Table 2. Knowing which reforming and cracking agents are present in the raw gas used, as well as the nature of the carbon-containing products obtained after the upgrading, one can determine whether H^* or O^* take part in the reactions. From this, the decomposition reactions that occur are determined. For example, the formation of smaller tar/light HC (C_xH_y) indicates an interaction between C^* and H^* . Thereby, the effect of either the steam dealkylation or the hydro-cracking reaction is revealed, since H^* originate from steam and/or H_2 . In the same way, the reaction of C^* with O^* to produce CO/CO_2 reflects either the steam reforming reaction or dry reforming reaction, since O^* originate from steam and/or CO_2 .

In the present work, the contributions of the decomposition reactions in the upgrading process of the Chalmers raw gas using an ilmenite catalyst were investigated. To study the different decomposition reactions individually and also simultaneously, synthetic reactant gas mixtures that mimic the composition of the Chalmers raw gas were used in the experiments. This raw gas contains a high content of steam, so the steam reforming reactions are expected to play key roles. Thus, the steam reforming reactions of representative tar and light HC components

were investigated individually, to examine the individual effects of these reactions. Subsequently, these experiments were repeated with the addition of H_2 and CO_2 to the reactant gas mixtures, to investigate the steam reforming reactions in the presence of these species. Therefrom, the contributions of the hydro-cracking and dry reforming reactions could be estimated. It is noteworthy that in the given context, the thermal cracking reaction was ignored in relation to other decomposition reactions, as reforming and cracking agents were present in excess in the reaction environment. Furthermore, as a catalyst was used, these agents were expected to be converted into reactive intermediates that would participate in the conversion of tar and light HC.

A kinetic model that describes the evolution of tar and light HC during the catalytic upgrading of raw gas was developed based on the formulated mechanism. The rate expressions for the conversion of tar and light HC were formulated using the rate-determining steps defined in the mechanism, as well as the distributions of CO/CO_2 and smaller tar/light HC as the products of the destruction of the parent tar/light HC. The contributions of the different decomposition reactions to the conversion of tar and light HC discussed above were used as an input to the model. Indeed, as the contributions of different decomposition reactions are known, it is possible to identify the extents to which the parent tar/light HC are converted into CO/CO_2 and into smaller tar/light HC. Details of the model are presented separately in Chapter 4.

3.2.2. Towards larger products

The mutual interaction of C^* in Figure 5 reflects the growth of PAH tar during the raw gas upgrading. This also reflects the growth of PAH tar during the tertiary conversion stage of biomass gasification, as discussed in Section 2.1. Particularly for biomass steam gasification, where steam is used as the gasifying agent and consequently, H_2 is produced from the WGS reaction, which is in addition to the steam and H_2 produced from the degradation of biomass, the reaction environment in the gasifier has potentially a surplus of H^* . The presence of H^* is known to limit the formation of relatively heavier products, as mentioned in Section 2.3. Thus, the idea is to utilize the available H^* source to suppress the mutual interactions of C^* , thereby reducing the growth of PAH tar during the tertiary conversion stage of biomass steam gasification. It is worth noting that during the tertiary conversion stage, the formation of C_2H_2 is important, thus, there is a possibility that C^* combine with C_2H_2 to create larger C^* , which also contributes to the growth of PAH tar as earlier mentioned. However, this interaction is prevented, if C^* already react with the available H^* .

In the present work, this idea of utilizing the steam and H_2 available in the reaction environment of biomass steam gasification to reduce the growth of PAH tar was evaluated in relation to different levels of process severity. In the conducted experiments, a slipstream of the raw gas produced in the Chalmers gasifier was extracted and fed into a reactor located downstream of the gasifier. In the downstream reactor, the raw gas was upgraded under

different process severities, to examine the changes in the tar and permanent gases. Using this downstream approach, the authentic reaction environment and the entire aromatic-tar spectrum involved in the gasification process is considered, which is more realistic than, for example, the approach of using synthetic gas mixtures that mimic a raw gas and contain specific monocyclic aromatics as PAH precursor models.

4. A kinetic model for catalytic raw gas upgrading

4.1. Description of the model

The model takes into account all the tar and light HC compounds present in the Chalmers raw gas. The tar and light HC are divided into eight groups (denoted C1–C8) that are: phenolic and oxygen-containing compounds (C1); benzene (C2); 1-ring compounds (excluding benzene) (C3); naphthalene (C4); 2-ring compounds (excluding naphthalene) (C5); ≥ 3 -ring compounds (C6); light HC in the range of C₂ to C₅ carbons (C7); and methane (C8). The components included in the presented groups can be found in **Paper I**. It is worth noting that phenolic and oxygen-containing compounds are treated as an individual group. Given that this group is taken into consideration, the chemical formula for tar stated above in Figure 3 is now re-written as C_{x_i}H_{y_i}O_{z_i} corresponding to group C_i. The light HC group is represented by its general chemical formula C_{x_i}H_{y_i}. Based on the tar and light HC compositions in the raw gas, the chemical formulas of C_{x_i}H_{y_i}O_{z_i}/C_{x_i}H_{y_i} for the tar/light HC groups C_i are derived.

A pseudo-tar, CH_mO_n, is introduced to represent all the tar and light HC produced *in situ*, i.e., CH_mO_n is produced from the destruction of tar and light HC group C_i. The values of *m* and *n* in CH_mO_n are derived from the contents of carbon, hydrogen, and oxygen in the upgraded gas, excluding CO, CO₂, and H₂. The parameter *w_i* (0 ≤ *w_i* ≤ *x_i*) is introduced to the model, which represents the number of carbons in a C_i molecule that is converted to CH_mO_n. After formation, CH_mO_n is distributed to all the tar and light HC groups C_i with the distribution coefficient *p_i* corresponding to each group. The formation and distribution of the pseudo-tar CH_mO_n are visualized in Figure 6, in which the formation of oxidation products (CO/CO₂) from the conversion of a C_i molecule is also included.

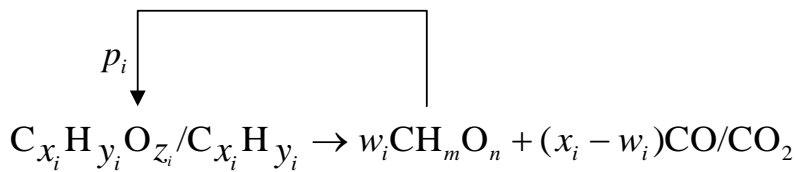


Figure 6. Scheme for the formation and distribution of pseudo-tar CH_mO_n.

An initial basic assumption is that the conversion of tar and light HC is controlled by kinetics. The rate expressions for the conversion of tar and light HC are derived based on the predefined rate-determining steps (i.e., elementary reactions R9–R11 discussed in Section 3.1), and the distribution of the pseudo-tar CH_mO_n. The rate expression for the conversion of group C_i in relation to the gas-solid contact time is as follows:

$$\begin{aligned} \frac{dX_{Ci}}{dt} &= -\frac{dX_{Ci}(9)}{dt} - \frac{dX_{Ci}(10)}{dt} - \frac{dX_{Ci}(11)}{dt} + p_i S \\ &= -k_{i9}X_{Ci} - k_{i10}X_{Ci}X_{H^*} - k_{i11}X_{Ci}X_{C^*} + p_i S \end{aligned} \quad \text{Eq. (1)}$$

where X_{Ci} is the mole fraction of group Ci [-], X_{H^*} is the mole fraction of hydrogen intermediate H^* [-], X_{C^*} is the mole fraction of carbon-containing intermediate C^* [-], k_{i9} , k_{i10} , and k_{i11} are the pseudo rate coefficients of elementary reactions R9–R11 with respect to group Ci [s^{-1}], p_i is the distribution coefficient for group Ci [-], and S is the total rate of CH_mO_n formation [s^{-1}], $S = \sum_i w_i(k_{i9}X_{Ci} + k_{i10}X_{Ci}X_{H^*} + k_{i11}X_{Ci}X_{C^*})$.

X_{C^*} , X_{H^*} are defined further as follows. The maximum rate of C^* formation can be estimated from elementary reaction R9 according to:

$$\frac{dX_{C^*}}{dt} = 2 \sum_i k_{i9}X_{Ci} \quad \text{Eq. (2)}$$

For a characteristic time-step $\Delta\tau$, the mole fraction X_{Ci} in Eq. (2) is assumed to be constant. The concentration of the reactive intermediates is also assumed to be constant throughout the reactions, as the reactive intermediates react immediately after formation [87]. Under these assumptions, Eq. (2) can be integrated as follows:

$$X_{C^*} = 2\Delta\tau \sum_i k_{i9}X_{Ci} \quad \text{Eq. (3)}$$

Using X_{C^*} from Eq. (3) and further introducing k'_{i11} to replace $k_{i11}\Delta\tau$, Eq. (1) can be rewritten as:

$$\frac{dX_{Ci}}{dt} = -k_{i9}X_{Ci} - k_{i10}X_{Ci}X_{H^*} - 2k'_{i11}X_{Ci} \sum_i k_{i9}X_{Ci} + p_i S \quad \text{Eq. (4)}$$

For the case in which steam and H_2 dissociate significantly and reach equilibrium, which is applied in the cases of catalysts that induce the WGS reaction, the mole fraction of H^* is derived from the expression of the equilibrium constant for elementary reaction R7, and Eq. (4) can be further written as:

$$\frac{dX_{Ci}}{dt} = -k_{i9}X_{Ci} - k'_{i10}X_{Ci}X_{H_2}^{0.5} - 2k'_{i11}X_{Ci} \sum_i k_{i9}X_{Ci} + p_i S \quad \text{Eq. (5)}$$

4.2. Empirical model coefficients representing product distribution

The empirical coefficients of the model, i.e., w_i , and p_i , describe the product distribution of the destruction of tar and light HC. As specified in Figure 6, when a molecule of $C_{x_i}H_{y_i}O_{z_i}$ or $C_{x_i}H_{y_i}$ is degraded, w_i carbon atoms are converted into CH_mO_n , and the remainder of the carbon atoms, i.e., $(x_i - w_i)$, is converted into CO/CO₂. In order to estimate the extents to which the parent tar and light HC are converted into other tar/light HC species and into CO/CO₂, knowledge of the contributions of the different decomposition reactions to the given upgrading process is required, as mentioned earlier. To compare the different tar and light HC groups in term of the product selectivity derived from their destruction, the ratio w_i/x_i is used instead. In relative

terms, branched aromatic tars have higher w_i/x_i values than non-branched aromatic tars, since the branched molecules are readily degraded at the side-chains to produce non-branched molecules [35, 43, 48].

The distribution coefficient p_i represents the relative dominances of the different tar and light HC groups produced *in situ*. The tar and light HC groups that are more stable have higher p_i values, since these stable species can be produced at significant levels from the less-stable species, as discussed in Section 2.2 [35, 43]. Thus, naphthalene, benzene, and CH_4 have higher p_i values than phenolic and oxygen-containing compounds, 2-ring compounds, 1-ring compounds, and C_{2-5}H_y . For the upgrading process in which the formation of relatively larger tar compounds is negligible, such as the process that takes place in a reaction environment containing a high content of steam, the natures of the tar and light HC produced *in situ* mainly depend on the molecular structures of the parent tar and light HC, respectively, in the raw gas used. The value range for the p_i input to the model calculation can be estimated based on the compositions and the molecular structures of the tar and light HC present in the raw gas.

5. Experimental section

5.1. Gasifier operation and raw gas properties

5.1.1. Gasifier operation

To the 12-MW_{th} boiler installed at Chalmers University of Technology, an indirect biomass gasifier is coupled to create a dual fluidized bed gasifier, as shown in Figure 7.

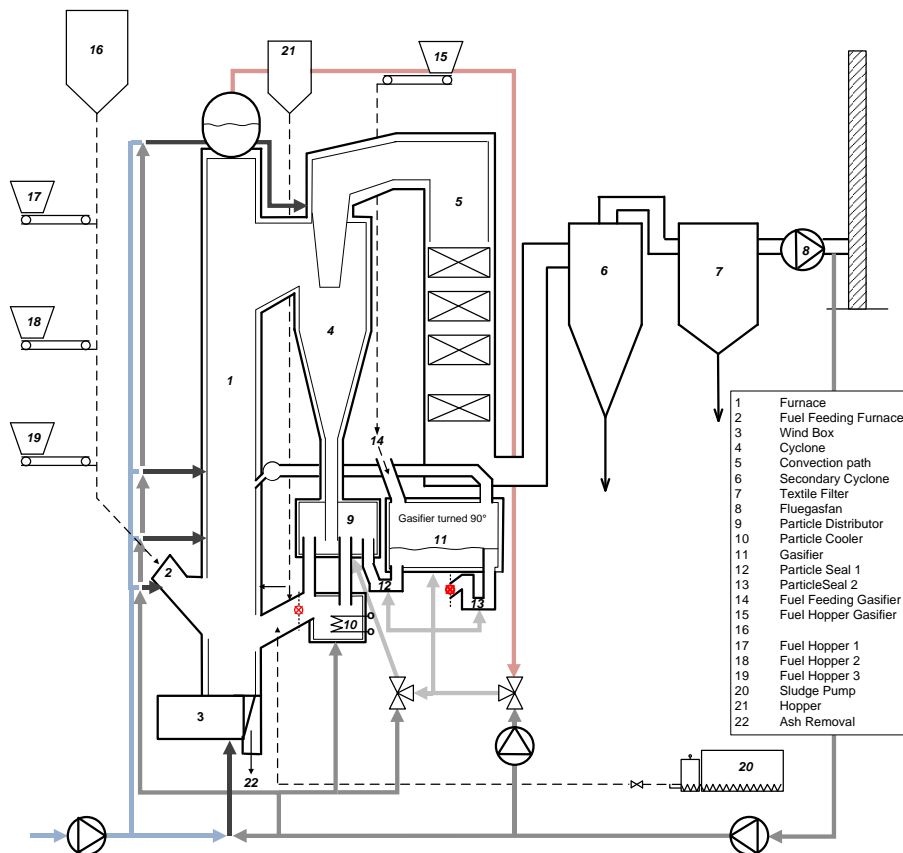


Figure 7. Schematic of the Chalmers combustion-gasifier unit.

The fuel feed to the gasifier accounts for about 25% of the total fuel load to the whole combustion-gasification unit. As the boiler is intended to be used to produce hot water for district heating at the Chalmers campus, excess fuel is fed to the boiler. Thus, the heat demand of the gasifier is always fulfilled, irrespective of the operating conditions of the gasifier. Further details of the Chalmers unit are available elsewhere [5, 11, 99]. The conditions used for operating the gasifier in this work are summarized in Table 3.

Table 3. Operating conditions for the gasifier.

Bed material	Silica sand
Total bed inventory (tonne)	3
Temperature (°C)	820
Wood pellet flow-rate (kg/h)	300
Steam flow-rate for fluidization in the gasifier (kg/h)	160
Raw gas residence time (s)	~5

5.1.2. Raw gas properties

The raw gas contained approximately 60 vol% of steam [5]. The permanent gas composition was analyzed online using the Rosemount NGA 2000 Multi-Component Gas Analyzer and a micro-gas chromatography system (micro-GC; Varian 4900). The NGA analyzer measures the concentrations of H₂, CO, CO₂, CH₄, and O₂. The micro-GC, which is equipped with a molecular sieve 5A column and a PoraPLOT Q column that uses Ar and He as carrier gases, measures the concentrations of H₂, CO, CO₂, CH₄, C₂H₂, C₂H₄, C₂H₆, C₃H₆, C₃H₈, N₂, O₂, and He. The composition of the permanent gas is presented in Table 4. In addition to the data provided in the table, C₂H₄ accounts for approximately 80% of the light HC in the range of C₂–C₃ carbons. Under the employed gasifier operating conditions, the yields of light HC in the range of C₄–C₅ carbons were negligible [65].

Table 4. Permanent gas composition (vol%).

H ₂	CO	CO ₂	CH ₄	C ₂₋₃ H _y	N ₂
28.4	28.7	19.3	12.2	4.9	6.5

For the tar sampling, the solid-phase adsorption (SPA) method was employed, which uses dual-layer, solid-phase extraction columns that contain a layer of aminopropyl-bonded silica and a layer of activated carbon (Supelclean ENVI-Carb/NH₂ SPE tube; Sigma-Aldrich). The presence of the activated carbon layer allows efficient quantification of light tar components, such as benzene, toluene, xylene, and styrene, which are additional to the heavier components that can be captured efficiently by the aminopropyl-bonded silica layer. The detailed procedures for extracting, preserving, and eluting the SPA samples, and the setup for gas chromatography with flame ionization detector (GC-FID) method for tar analysis are described elsewhere [100]. The tar content of the dry raw gas was about 62 g/Nm³. The tar composition is depicted in Figure 8. In the figure, the tar components are presented in the order of their retention times in the GC-FID

chromatograms. Furthermore, the ‘unknown tar’ category refers to the total amount of tar components that were detected by the employed GC-FID but only at very low levels, and as a consequence, they were not included in the standard tar compounds predefined in the GC-FID method. When data regarding the compositions of the different tar groups were required, the unknown tars were assigned to the most plausible known tar groups based on their retention times in the GC-FID chromatograms. It is noteworthy that the applied methods for measuring the permanent gases and tar ensure identification of all the potential carbon-containing products of the raw gas [65, 100].

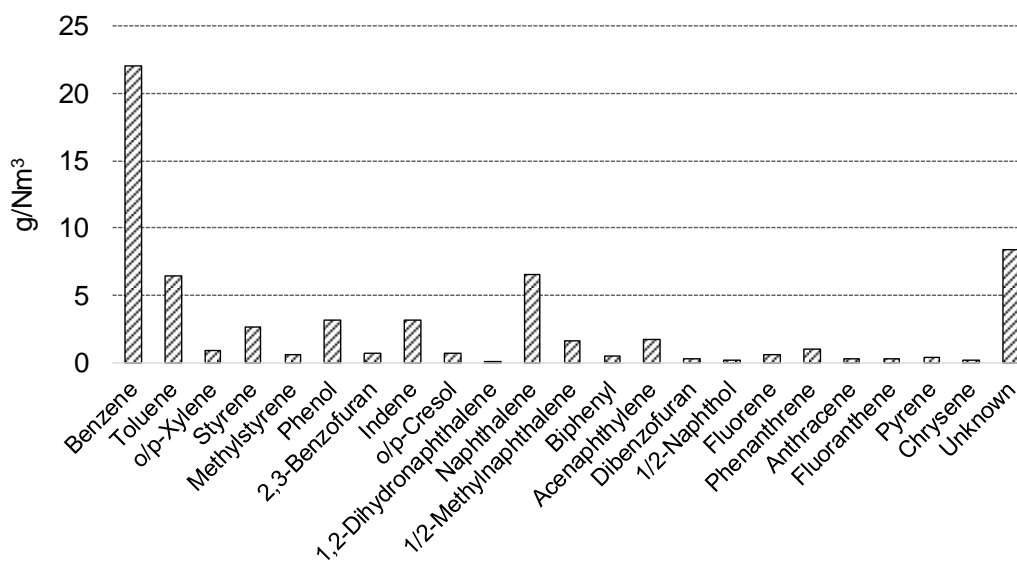


Figure 8. Typical tar content (g/Nm³) of the Chalmers raw gas.

5.2. Gas upgrading experiments

5.2.1. Activation of ilmenite

The activity of ilmenite is largely attributed to its iron content [11, 60, 99, 101]. To induce the reactivity of fresh ilmenite, activation is required. During this activation, ilmenite is exposed to alternating oxidizing and reducing conditions at a temperature of at least 800°C, to enhance the porosity (i.e., the specific surface area) and to trigger the migration of iron to the particle surface [102, 103]. It should be emphasized that ilmenite possesses both oxygen transport and catalytic capacities. The dominant activity is manifested depending on the redox state of the iron: oxidized state Fe⁺³ contributes most to oxygen transport capacity and the reduced iron species, such as Fe⁺² and Fe⁰, are the most active in terms of catalytic activity. For ilmenite to function as a catalyst and not as an oxygen carrier, the activation process needs to ensure that the iron in ilmenite is in its reduced form [11, 60, 99, 101].

In the experiments conducted in the present work, fresh ilmenite and process-activated ilmenite were used. The fresh ilmenite was activated during the course of the gas upgrading experiments. The activation was performed at 800–900°C, during which an oxidation gas stream (5 vol% O₂ and 95 vol% N₂) and a reduction gas stream (10% CO, 10% H₂, and 80 vol% N₂) were alternately fed to the reactor. The process-activated ilmenite was ilmenite that had previously been activated during a time-on-stream of approximately 1 day in the Chalmers boiler, which at the time was operated at about 900°C. The ilmenite was exposed to the alternating oxidizing and reducing conditions of the combustion process. Ash elements (such as calcium and potassium) that originated from the biomass fed to the boiler were deposited on the surfaces of the ilmenite particles, which could then contribute to enhancing the catalytic activity of the process-activated ilmenite [13, 104, 105].

5.2.2. Experimental setups

Two experimental setups were used (Figure 9 and 10). The setup in Figure 9 was used for investigations with synthetic reactant gases (**Paper II**). The setup in Figure 10 was used for investigations with raw gas produced in the Chalmers gasifier (**Papers I, III and IV**).

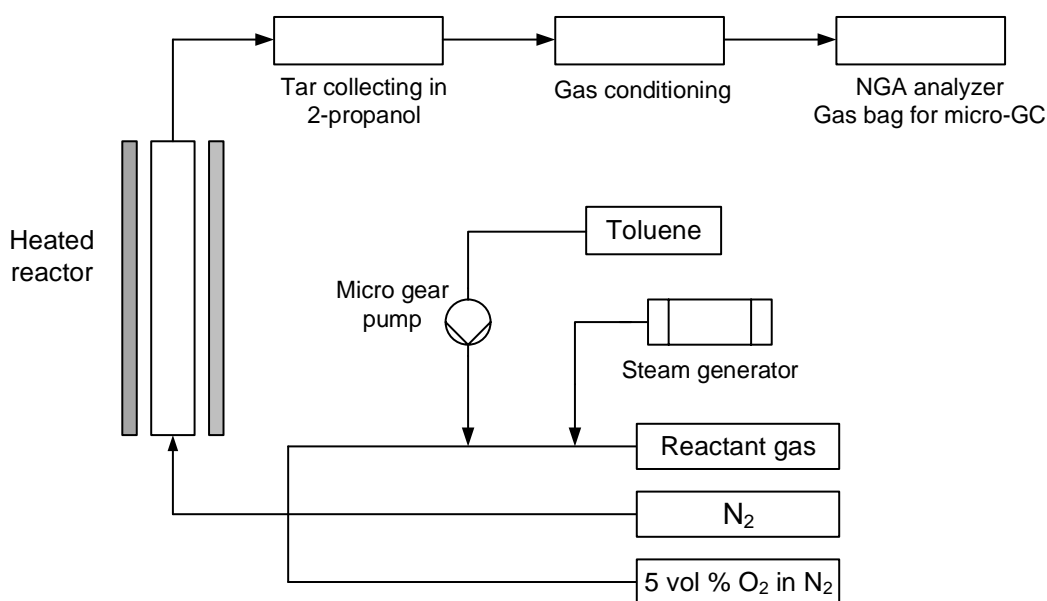


Figure 9. Experimental setup for investigations with synthetic reactant gas mixtures.

The main part of the experimental setup in Figure 9 is a laboratory-scale, quartz glass fluidized bed reactor. The bed material used was fresh ilmenite (125–180 μm), which was activated during the course of the experiments. The operating temperature range of 750–900°C was investigated. The experiments were performed in cycles that consisted of three successive stages, namely the reduction, inert, and oxidation stages. For each experiment, two cycles were carried out to ensure the reproducibility of the experiment. The main focus was the reduction stage, during

which the synthetic reactant gas mixtures were fed to the reactor. Steam represented about 50 vol% of the reactant gas mixtures used. The oxidation stage, which employed a mixture of 5 vol% O₂ diluted in N₂, was carried out to regenerate the ilmenite from any carbon deposits. Between the reduction stage and the oxidation stage, the inert stage using pure N₂ was implemented to flush the reactor. In the experiments involving toluene injection, the tar in the product gas exiting the reactor was collected using 2-propanol impingers placed in a cold bath. The samples of 2-propanol were further analyzed by GC-FID to quantify the levels of remaining toluene and other tar compounds formed during the reduction stage.

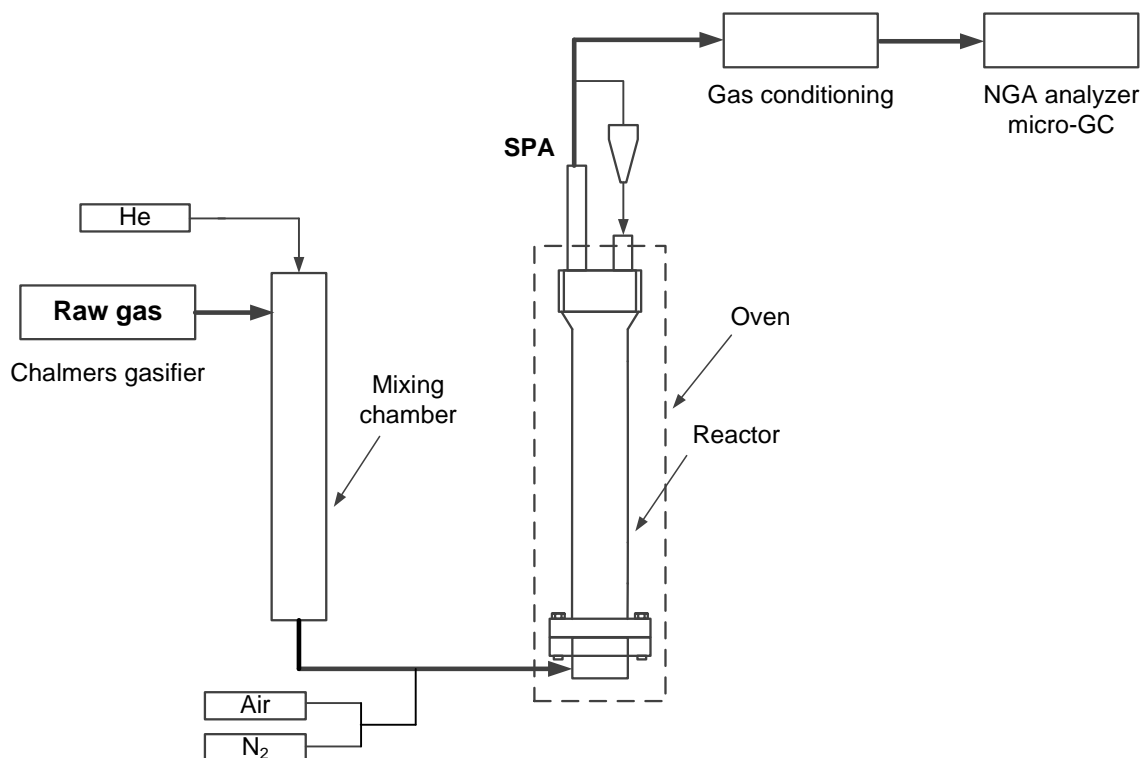


Figure 10. Experimental setup for the investigations with Chalmers raw gas.

The main part of the experimental setup in Figure 10 is a bench-scale, bubbling fluidized bed reactor that is fed a slipstream of the Chalmers raw gas. The bed materials were silica sand and process-activated ilmenite, which were used to investigate the effects of different gas residence times and gas-solid contact times, respectively. For ilmenite, two particle size ranges (45–90 μm and 125–180 μm, hereinafter referred to as ‘ilmenite **A**’ and ‘ilmenite **B**’, respectively, in accordance with the Geldart classification of particles [106]) were investigated. For silica sand, the particle size range of 125–180 μm was used. The temperature range of 800–850°C, which corresponds to the operating temperature of fluidized bed gasifiers, was investigated.

The experiments were performed in batch mode. During the raw gas operation, a trace stream of He was added to the raw gas, to allow derivation of the flow rate of the upgraded gas exiting the reactor. The tar sampling for the upgraded gas at the outlet of the reactor was carried

out using the same method as was used for sampling the tar in the raw gas. After the conditioning step to remove steam and tar, the permanent gas composition was analyzed online using the NGA gas analyzer and the micro-GC. When required, air and N₂ were introduced into the reactor instead of the raw gas, so as to regenerate the bed material and flush the reactor, respectively. It is worth noting that the carbon deposited on the bed materials was determined from the amount of CO₂ produced during the regeneration of the bed materials after the operation with synthetic reactant gas or with the Chalmers raw gas in the two experimental setups.

6. Results and discussion

This chapter presents the main results obtained for the applications of the proposed mechanism and discusses these results. The results are outlined into Sections 6.1–6.3, which pertain to **Paper II**, **Papers I and III**, and **Paper IV**, respectively.

6.1. Contribution of decomposition reactions to the conversion of tar and light hydrocarbons

In the experiments that used the synthetic reactant gas mixtures of either C_2H_4 and steam or toluene and steam for investigating the steam reforming reactions, high production levels of CH_4 and benzene were observed, respectively, in addition to CO/CO_2 (details about these results can be found in **paper II**). This was the case despite the fact that the level of steam in the used synthetic reactant gas mixtures were sufficient for C_2H_4 and toluene to be completely converted into CO/CO_2 . The obtained results indicate the effect of complete steam reforming and steam dealkylation, and confirm that the catalytic activity of ilmenite under the studied conditions is not sufficient to eliminate CH_4 and benzene.

To evaluate the contributions of the hydro-cracking and dry reforming reactions, the natures of the products from the conversion of C_2H_4 and toluene were compared for the following cases: (i) C_2H_4 and toluene were decomposed mainly *via* steam reforming reactions; and (ii) in addition to steam reforming, it was possible for C_2H_4 and toluene to be decomposed *via* the hydro-cracking and dry reforming reactions, which could be enhanced by the WGS reaction. The results are shown in Figure 11 for C_2H_4 conversion and in Figure 12 for toluene conversion.

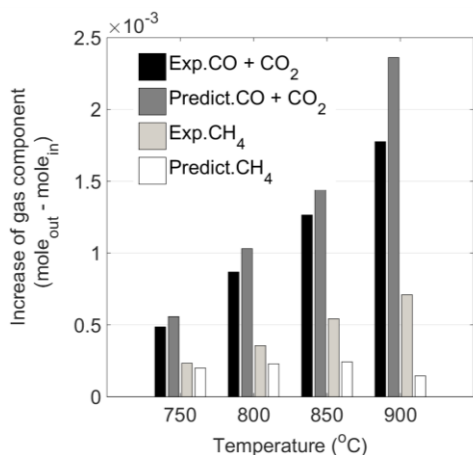


Figure 11. Experimental (Exp.) data and predicted (Predict.) data showing the increases in the levels of CO plus CO₂, and of CH₄ in the experiments using synthetic reactant gas mixtures that consisted of C₂H₄, CH₄, CO, CO₂, H₂, and steam. The Predict. data were calculated with the assumption that only steam reforming reactions were occurring.

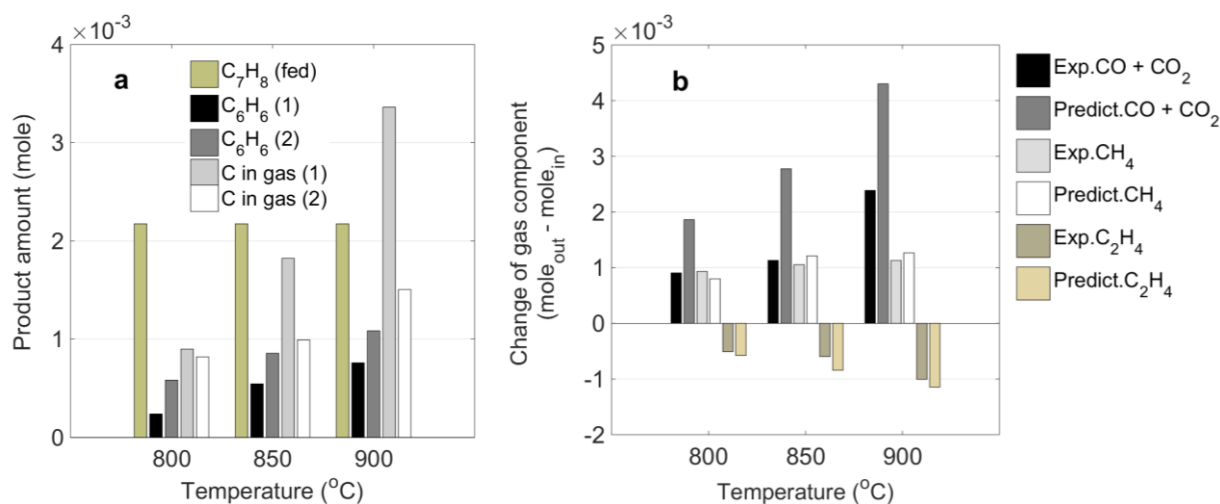


Figure 12, a-b. **a)** Changes in the levels of benzene and total carbon in the permanent product gas obtained for the experiments using synthetic reactant gas mixtures that consisted of: (1) toluene and steam; and (2) toluene, C₂H₄, CH₄, CO, CO₂, H₂, and steam. **b)** Experimental (Exp.) data and predicted (Predict.) data for increases in the levels of CO plus CO₂, and of CH₄, and for decreases in the levels of C₂H₄ in the experiments using the synthetic reactant gas mixture (2). The Predict. data were calculated with the assumption that only steam reforming reactions were occurring.

The results in Figure 11 show that the actual increases in the levels of CO plus CO₂ were lower than the predicted values, and this difference became more pronounced as the reactor temperature was increased. However, the opposite trend was observed for the levels of CH₄. The results in Figure 12a show that the levels of benzene produced from toluene conversion were

higher for the reactant gas mixture that consisted of toluene, C₂H₄, CH₄, CO, CO₂, H₂, and steam than for the reactant gas mixture that consisted only of toluene and steam. However, the changes in the amounts of carbon in the permanent product gases followed the opposite trend. In Figure 12b, the most significant differences between the experimental and predicted results were noted for CO plus CO₂, whereby the increases observed experimentally were lower than the predicted increases, and this difference became more prominent as the reactor temperature was increased. Overall, the observations of C₂H₄ conversion and toluene conversion indicate that the production of carbon-containing products deviates towards more HC products and fewer oxidation products, as H₂ was present in the reactant gas mixture used and H₂ was produced due to the WGS reaction. These results reveal the effect of the hydro-cracking reaction. That the presence of CO₂ in the reactant gas mixture and the CO₂ produced from the WGS reaction did not direct the process towards more oxidation products indicates that the dry reforming reaction was insignificant. For the given upgrading process, complete steam reforming, steam dealkylation, and hydro-cracking reactions are important, whereas the dry reforming reaction is insignificant. Furthermore, the *in situ* formation of other tar and light HC that are more stable than the parent tar and light HC, respectively, is important.

6.2. Evaluation of the kinetic model

6.2.1. Composition of upgraded gas

The model presented in Chapter 4 was fitted to the experimental data, to estimate the composition of the upgraded gas as a function of the gas-solid contact time. Typical results from the model calculation are presented in Figure 13–15 for ilmenite **B** at 800°C, ilmenite **B** at 850°C, and ilmenite **A** at 850°C. In these figures, the ‘measured compositions’ are the experimental data, and the ‘calculated compositions’ are obtained by fitting the kinetic model to the experimental data.

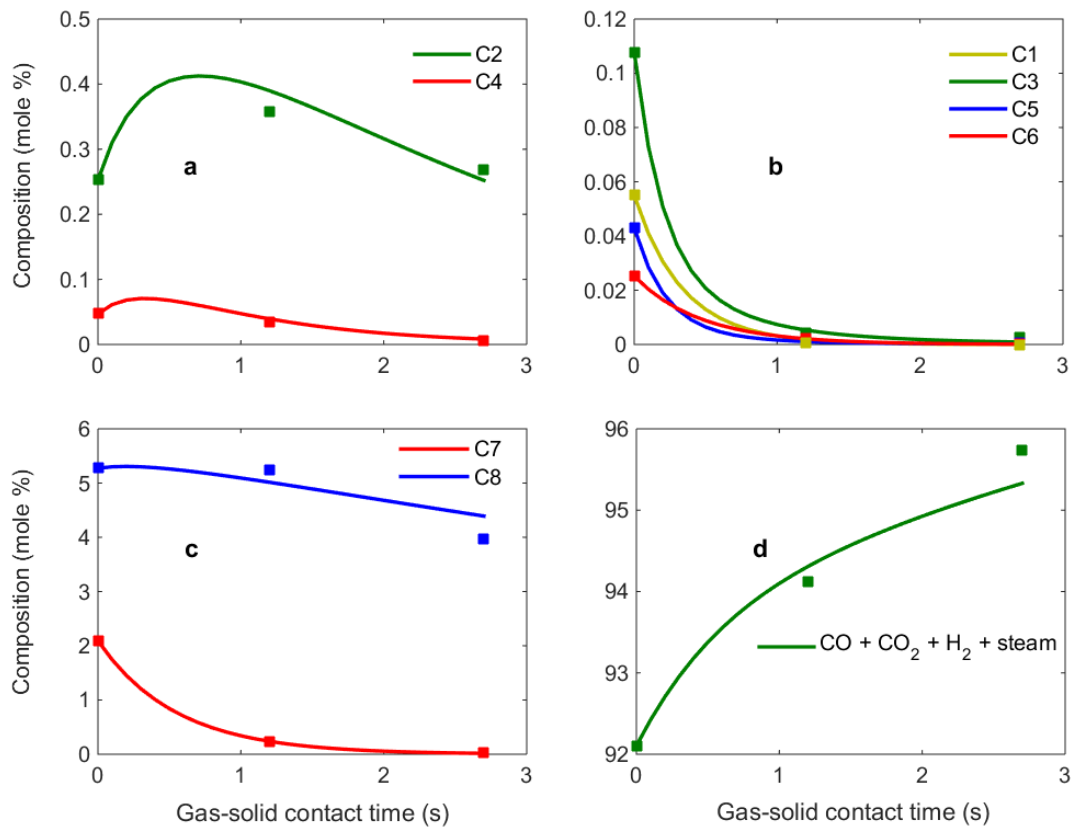


Figure 13, a–d. Calculated (lines) and measured (markers) compositions of the upgraded gas for ilmenite **B** at 800°C.

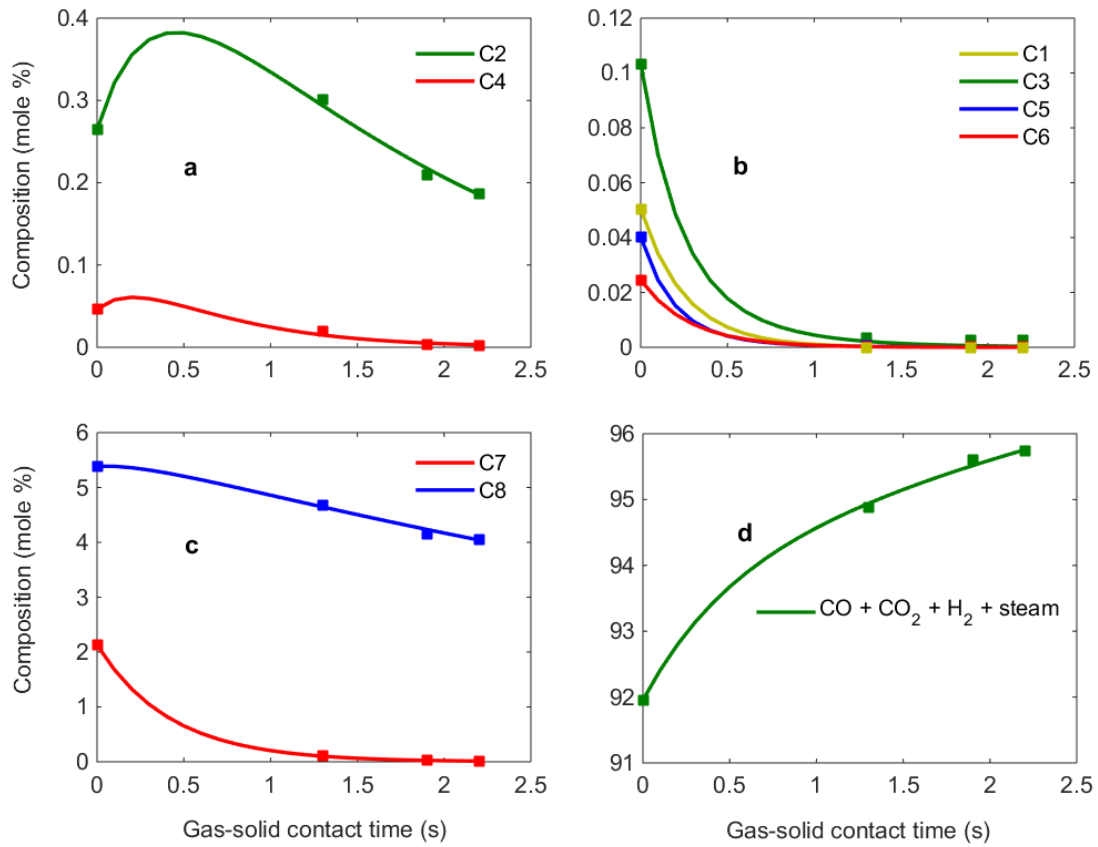


Figure 14, a–d. Calculated (lines) and measured (markers) compositions of the upgraded gas for ilmenite **B** at 850°C.

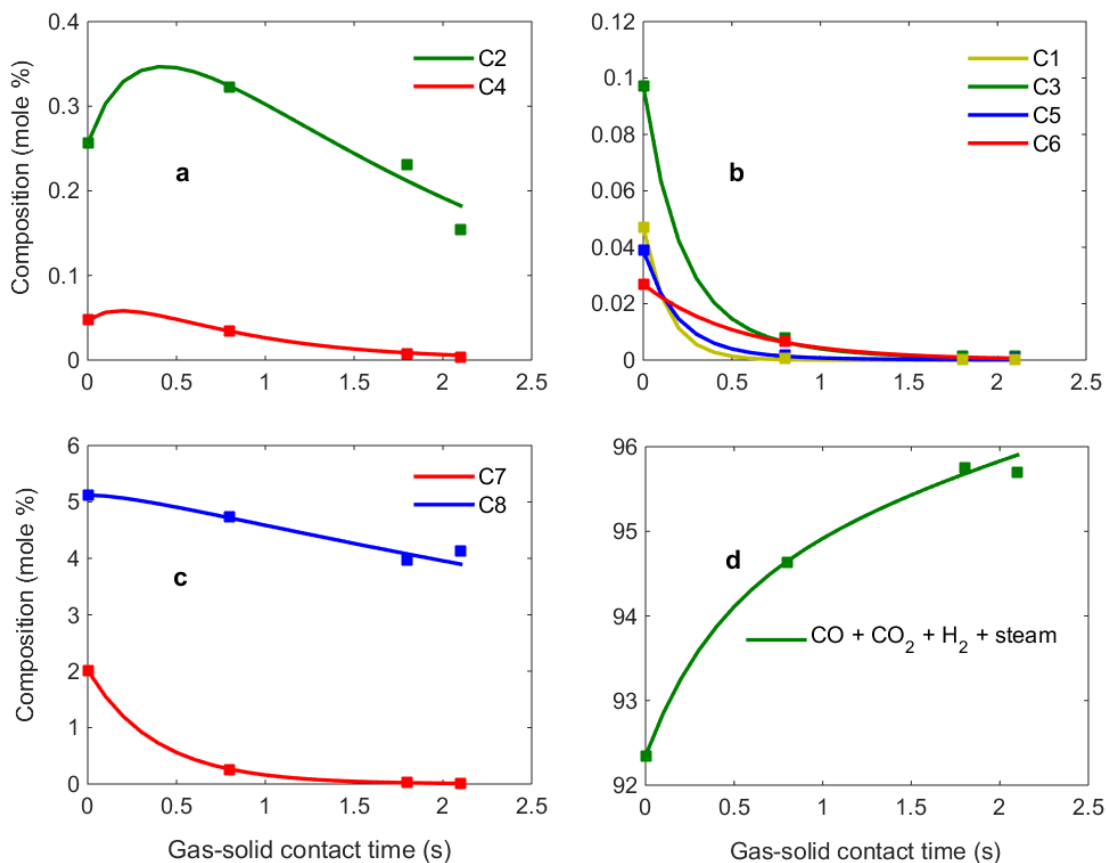


Figure 15, a–d. Calculated (lines) and measured (markers) compositions of the upgraded gas for ilmenite **A** at 850°C.

The model results with optimized empirical coefficients approached the measured compositions, as shown in Figure 13–15. This indicates that the model is capable of describing the upgrading process. Lower concentrations of phenolic and oxygen-containing compounds (C1), 1-ring compounds (C3), 2-ring compounds (C5), and ≥ 3 -ring compounds (C6) were achieved as the contact time increased. The destruction of these tar groups produced benzene (C2) and naphthalene (C4), resulting in increases in the levels of C2 and C4. For the light HC, $C_{2-3}H_y$ (C7) was almost completely eliminated at the longest gas-solid contact time obtained for each investigated case. In contrast, methane (C8) persisted at a relatively high level in the upgraded gas, due to the conversion of tar and $C_{2-3}H_y$ producing CH_4 . As the contact time increased, naphthalene, benzene, and CH_4 were the main tar and light HC groups in the upgraded gas. From the obtained evolutionary profiles, a conversion network for the tar and light HC groups is formulated (Figure 16).

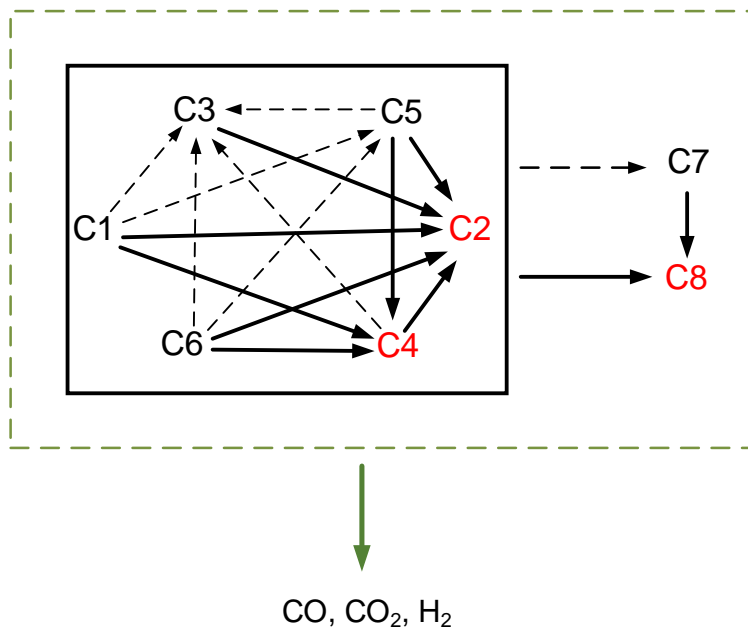


Figure 16. Proposed conversion network for tar and light HC groups.

In general, in the conversion network, the destruction of the heavier tar/light HC groups produces relatively lighter species. $C_{2-3}H_y$ and CH_4 can be produced from all the tar groups, and the destruction of $C_{2-3}H_y$ can result in the formation of CH_4 . The conversion routes that produce naphthalene, benzene, and CH_4 are represented as the most important in the putative network using solid lines. Syngas (CO , CO_2 , and H_2) is the final product of the conversion network.

Effects of particle size and temperature on the conversion of tar and light HC

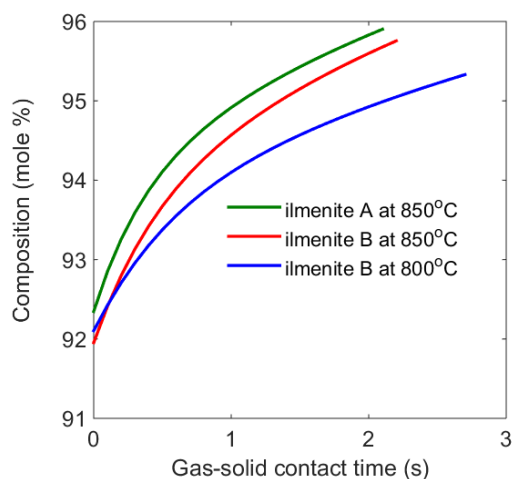


Figure 17. Aggregated compositions of CO , CO_2 , H_2 and steam for different gas-solid contact times in the reactor.

To compare the effects of particle size and temperature on the conversion of tar and light HC, the calculated sums of the CO, CO₂, H₂ and steam compositions in the three studied cases presented in Figure 13–15 are once more presented in Figure 17. For the same gas-solid contact time, the sums in order of magnitude for the given conditions are: ilmenite **A** at 850°C > ilmenite **B** at 850°C > ilmenite **B** at 800°C. Comparing ilmenites **A** and **B** at 850°C, the difference in the summed compositions of CO, CO₂, H₂ and steam was most likely due to the differences in the compositions of the raw gases used. This suggests that the effect of particle size is negligible. Presumably, if the reactions were controlled by mass transfer, the reaction rates would be proportional to the external catalytic surface. When **A**-type particles were replaced with **B**-type particles, the total external catalytic surface decreased by several orders of magnitude. Thus, the effect of particle size was expected to be more significant than what was observed. The obtained results support the assumption made for the model that the reactions are controlled by kinetics (and not by mass transfer) within the investigated ranges of particle sizes and process severities. The effect of temperature was clearly evident as the difference between the summed compositions of CO, CO₂, H₂ and steam for ilmenite **B** at 850°C and at 800°C; this difference became more pronounced as the gas-solid contact time increased.

Validation of calculated data

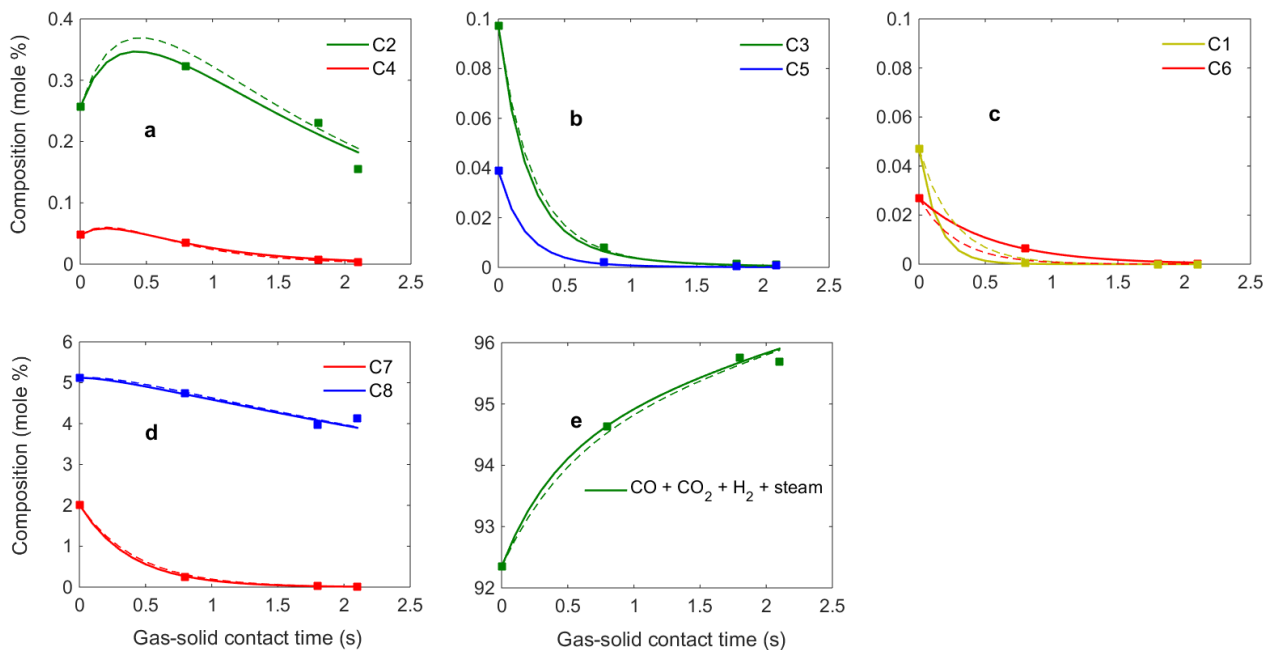


Figure 18, a–e. Calculated (lines) and measured (marker) compositions of the upgraded gas for ilmenite **A** at 850°C. The solid lines are taken from Figure 15, and the dashed lines show the data obtained using the empirical coefficients for ilmenite **B** at 850°C.

As the obtained results showed that the effect of particle size was negligible, the measured composition for ilmenite **A** at 850°C was used to validate the empirical coefficients for ilmenite **B**

at 850°C. The result is shown in Figure 18. The dashed lines represent the predicted compositions obtained using the coefficients for ilmenite **B** at 850°C. The solid lines are taken from Figure 15, which are presented once again for comparison. In the figure, the dashed lines and the solid lines almost overlap. Thus, the empirical coefficients for ilmenite **B** at 850°C are deemed to be validated. Relatively large deviations between the dashed line and solid line are observed for C1, C2, and C6, suggesting that the coefficients for ilmenite **B** at 850°C could be chosen even more appropriately, provided that additional experiments are conducted for ilmenite **B** at 850°C with shorter gas-solid contact times than those applied in the present work.

6.2.2. Activation energy of tar and light hydrocarbons

The numerical data from the model calculation revealed that the initial destruction of tar and light HC molecules triggered by the interactions of these tar and light HC molecules with the tar and light HC reactive intermediates is negligible, as compared with the total effect of the self-dissociation and the dissociation facilitated by the hydrogen intermediate H^* (cf. *Supporting Information* in **Paper III**). Therefore, the third term in Eq. (5) was neglected, and the rate expression for the conversion of group C_i was then reduced to: $\frac{dX_{Ci}}{dt} = -k_s \cdot X_{Ci} + p_i \cdot S$. Using this equation and the data for ilmenite **B** at 800°C and for ilmenite **B** at 850°C, the activation energies of the C_i groups were derived.

Table 5. Activation energies of the tar and light HC groups.

Group	E_a (kJ/mole)			
	This work	Literature values		
		Without catalyst	With catalyst	Lumped tar
C1: phenolic and oxygen-containing compounds	64	263 (<i>phenol, pyrolysis</i>) [107]	-	99 (<i>without catalyst</i>) [108]
C2: benzene	72	443 (<i>steam & H₂</i>) [48]	221 (<i>calcined dolomite, steam & H₂</i>) [49]	84 (<i>calcined dolomite</i>) [109] 58 (<i>commercial nickel-based</i>) [110]
C3: 1-ring compounds	11	274 (<i>toluene, steam & H₂</i>) [48]	91 (<i>toluene, coal char, steam</i>) [111] 196 (<i>toluene, Ni/olivine, steam</i>) [112]	
C4: naphthalene	73	350 (<i>steam & H₂</i>) [48]	71 (<i>coal char, steam</i>) [111]	
C5: 2-ring compounds	46	-	-	
C6: ≥ 3-ring compounds	110	-	-	
C7: light hydrocarbons $C_{2-3}H_y$	51	109 (<i>ethene, pyrolysis</i>) [108]	-	
C8: methane	94	126 (<i>steam</i>) [113]	62 (<i>commercial nickel-based, steam</i>) [110]	

The obtained values were compared to some relevant data reported in the literature, to preliminarily assess the reliability of the obtained values, as shown in Table 5. The literature data were selected based on the criterion that the tar components and reaction environments were, to some extent, comparable to those of the present work. The tar model, catalyst, and reaction environment used in the cited reports are briefly noted [48, 49, 107-113]. The comparison shows, to some extent, that the obtained values are reasonable. Specifically, the obtained values are in the range for kinetics-controlled reactions [114]. Thus, the assumption of the model that the conversion of tar and light HC is controlled by kinetics is once again supported.

It should be stressed that the performed estimation of the activation energies of the tar and light HC groups represents the first attempt to elucidate a potential of the model other than its ability to describe the raw gas upgrading process. For uses of activation energies derived from the model, e.g., to predict the compositions of the upgraded gas at temperatures for which experiments have not been conducted, significant efforts in future studies are required. For example, additional experiments need to be performed with shorter gas-solid contact times than those adopted in the present work, i.e., contact times of <1.2 s (*cf.* Figure 13 and 14), to ensure that the results obtained from fitting the model are more reliable within the contact time range of 0–1.2 s. Thereby, the activation energies could be derived more accurately, especially for the less-stable groups, which are converted more rapidly, e.g., group C3. Investigations to validate the calculated activation energies, and to examine the reaction conditions under which the activation energies are reliable are also needed.

Overall, the results obtained from the model evaluation confirm that the model captures the main features of the upgrading process. The first attempt to estimate the activation energies of the different tar and light HC groups using the proposed model has been carried out. The results obtained for process-activated ilmenite can be usefully applied to designing a catalytic raw gas upgrading process that uses this catalyst, particularly with respect to selecting the appropriate temperature, particle size, and gas-solid contact time. Regarding the use of ilmenite in a process operated under conditions similar to those of the present work, the calculated composition of the upgraded gas provides a way to follow the upgraded gas quality and the tar composition.

As the model allows flexibility in incorporating different features that are specific for different processes, further uses of the model under different operating conditions are encouraged. Indeed, depending on the operating conditions applied to the upgrading process, the model can be adapted to incorporate specific features. For example: (i) if the formation of carbon deposits and soot are important, carbon deposits and soot can be designated as tar groups, whereby they are included in the calculation; (ii) if the operating condition applied to the upgrading favors methanation and other Fischer-Tropsch reactions, the tar/light HC is formed *in situ* from the reactions of gas species, i.e., CO and H₂, in which case the rate S_{gas} (representing the rate of CH_mO_n formation from CO and H₂) is specified and incorporated into the term S ; and (iii) the

individual mole fractions of CO, H₂, and CO₂ in the upgraded gas can be calculated if the kinetic data for the WGS reaction are available for the studied catalysts.

6.3. Fate of PAH tar during the tertiary conversion of steam gasification of biomass

In Figure 19–22, the experiments were designated according to their main operating conditions. Thus, the names of the experiments using silica sand include the values of gas residence time in the reactor, while the names of the experiments using ilmenite include the gas-solid contact times in the ilmenite bed. For example, the name ‘S800R3.3’ indicates that the experiment was conducted with silica sand as the bed material, at 800°C, and with a gas residence time of 3.3 s. In the same way, the name ‘I850C0.8’ indicates that the experiment was conducted with ilmenite as the bed material, at 850°C, and with a gas-solid contact time of 0.8 s.

6.3.1. Contributions of thermal and catalytic effects to process severity

Figure 19 and 20 show the tar compositions and tar decomposition efficiencies for the experiments conducted at 800°C and 850°C, respectively.

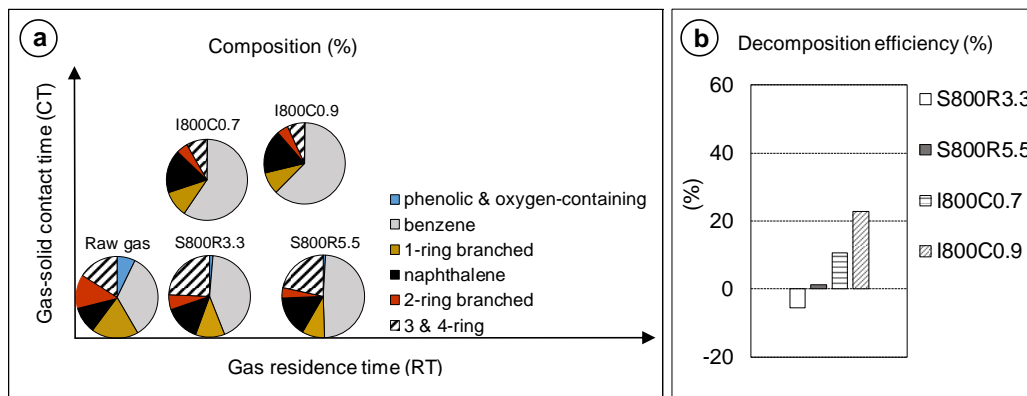


Figure 19, a–b. Tar composition (%) and tar decomposition efficiency (%) $[(g/kg_{daf\ fuel})_{raw\ gas} - (g/kg_{daf\ fuel})_{upgraded\ gas}] / (g/kg_{daf\ fuel})_{raw\ gas}$ for experiments conducted at 800°C.

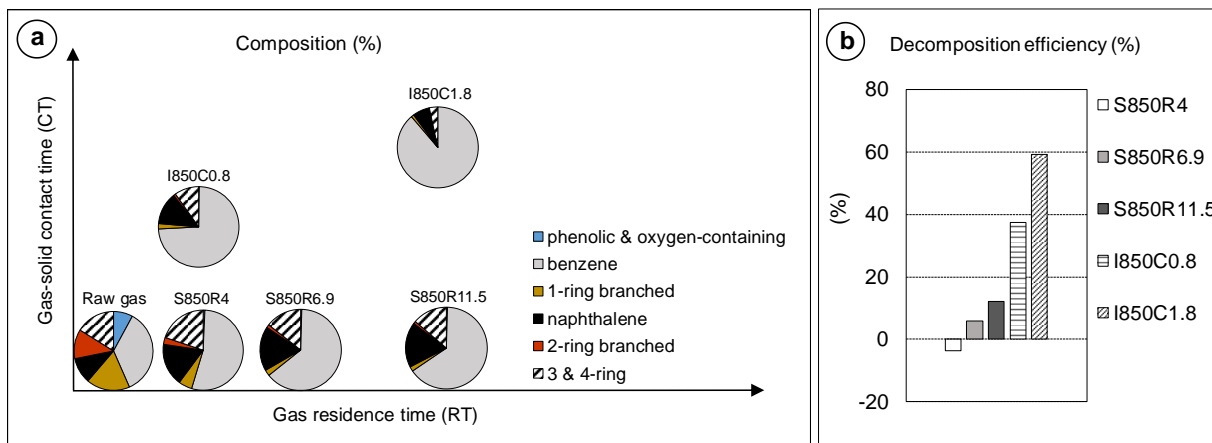


Figure 20, a–b. Tar composition (%) and tar decomposition efficiency (%) $[(\text{g}/\text{kg}_{\text{daf fuel}})_{\text{raw gas}} - (\text{g}/\text{kg}_{\text{daf fuel}})_{\text{upgraded gas}}]/(\text{g}/\text{kg}_{\text{daf fuel}})_{\text{raw gas}}$ for experiments conducted at 850°C.

In Figure 19a and 20a, the pie charts are positioned to correspond to the illustrated scales of the gas residence time and gas-solid contact time, which facilitates comparisons of the experiments in terms of the levels of these operating parameters. In general, following the increased gas residence time and gas-solid contact time, the increased composition of naphthalene and benzene, and decreased levels of phenolic and oxygen-containing, 1-ring, and 2-ring tar compounds were observed. In I850C0.8 and I850C1.8 where the process severity was relatively higher, the destruction of naphthalene to produce, for example, benzene became more significant as evidenced by the decreased composition of naphthalene and more considerable increase of benzene composition (see Figure 20a). In S800R3.3, S800R5.5 and S850R4, there were clear and noteworthy increases in the composition of 3 & 4-ring compounds, a phenomenon that was not seen in the ilmenite experiments.

The results for tar removal efficiency shown in Figure 19b and 20b reveal that in the ilmenite experiments, either the gas-solid contact time contributed to the tar decomposition or its contribution was several orders of magnitude higher than that of the gas residence time. This was identified by comparing ilmenite experiments and silica sand experiments with the same residence time levels, i.e., comparing I800C0.7 and S800R3.3, I800C0.9 and S800R5.5, I850C0.8 and S850R4, and I850C1.8 and S850R11.5. Furthermore, the presence of a gas-solid contact time, even at its lowest level, induced a considerably higher efficiency of decomposition than the cases in which only the gas residence time affected the tar decomposition, even at the highest gas residence time (i.e., comparing I800C0.7 and S800R5.5, and I850C0.8 and S850R11.5). Thus, the obtained results confirm that for the experiments discussed here, the catalytic effect contributes to process severity to a greater extent than does the thermal effect.

6.3.2. Growth of PAH tar

Figure 21 and 22 show the relative changes in the contents of the different tar components when comparing the upgraded gas to the raw gas for the silica sand experiments and ilmenite experiments, respectively.

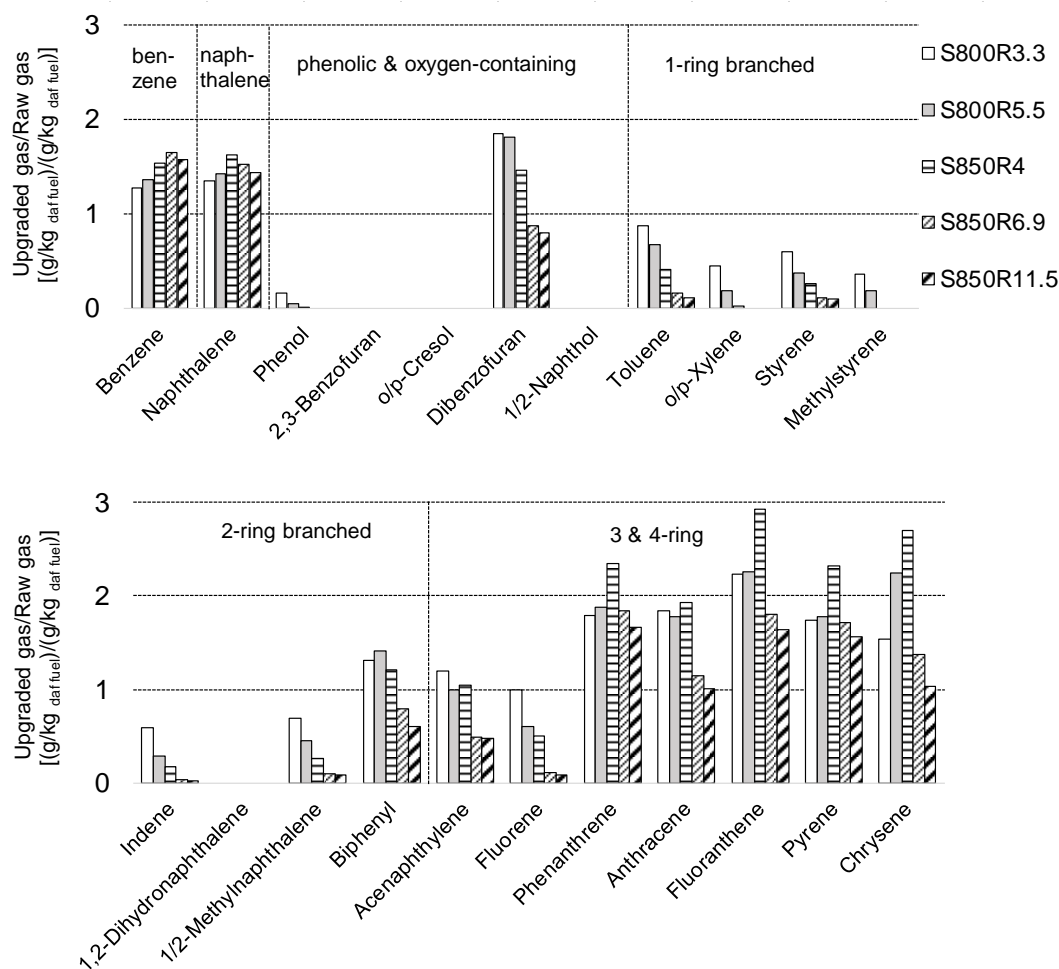


Figure 21. Relative changes in the contents of the different tar components, comparing upgraded gas to raw gas $[(\text{g/kg}_{\text{daf fuel}})_{\text{upgraded}}]/[(\text{g/kg}_{\text{daf fuel}})_{\text{raw}}]$ for the silica sand experiments.

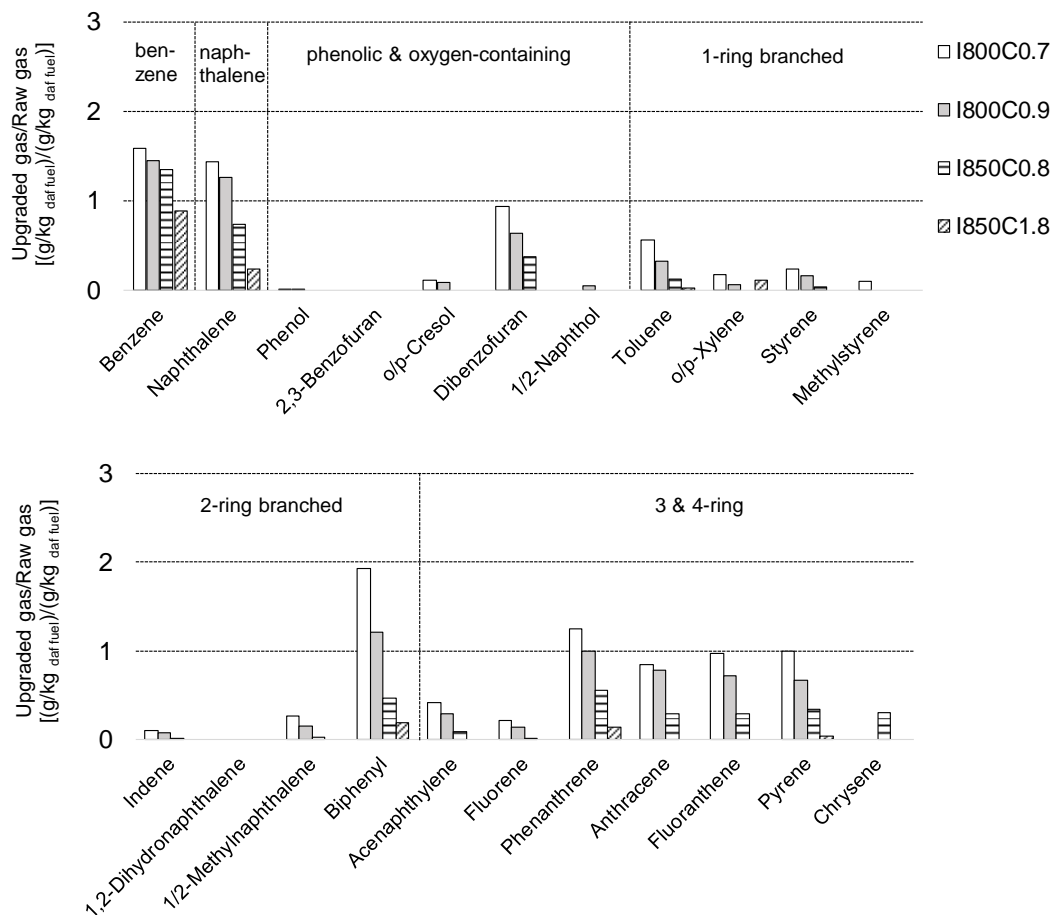


Figure 22. Relative changes in the contents of the different tar components comparing upgraded gas to raw gas $[(g/kg_{daf\ fuel})/(g/kg_{daf\ fuel})]$ for the ilmenite experiments.

In the silica sand experiments, at both investigated temperatures, increases in the levels of dibenzofuran, biphenyl, acenaphthylene, phenanthrene, anthracene, fluoranthene, pyrene, and chrysene were observed. These observations indicated that the growth of PAH tar from smaller tar species occurred. When the temperature was changed from 800°C to 850°C, there was a shift of less-stable tars (e.g., dibenzofuran and biphenyl) into more-stable tars (e.g., phenanthrene, anthracene, fluoranthene, pyrene, and chrysene that belong to 3 & 4-ring group). For S850R4, in that a relatively short residence time was applied, the increase in the level of phenanthrene, anthracene, fluoranthene, pyrene, and chrysene was strongest. At 850°C and following the increase in residence time, the increase of these tar components occurred to a lesser extent. In contrast to the silica sand experiments, when ilmenite was used as the bed material, there were only slightly increases in the levels of biphenyl and phenanthrene in I800C0.7 and I800C0.9. Based on these observations, and the contributions of the thermal effect and catalytic effect to the process severity discussed above, Figure 23 specifically visualizes the relationship between the content of 3 & 4-ring PAH tar in the upgraded gas and the process severity.

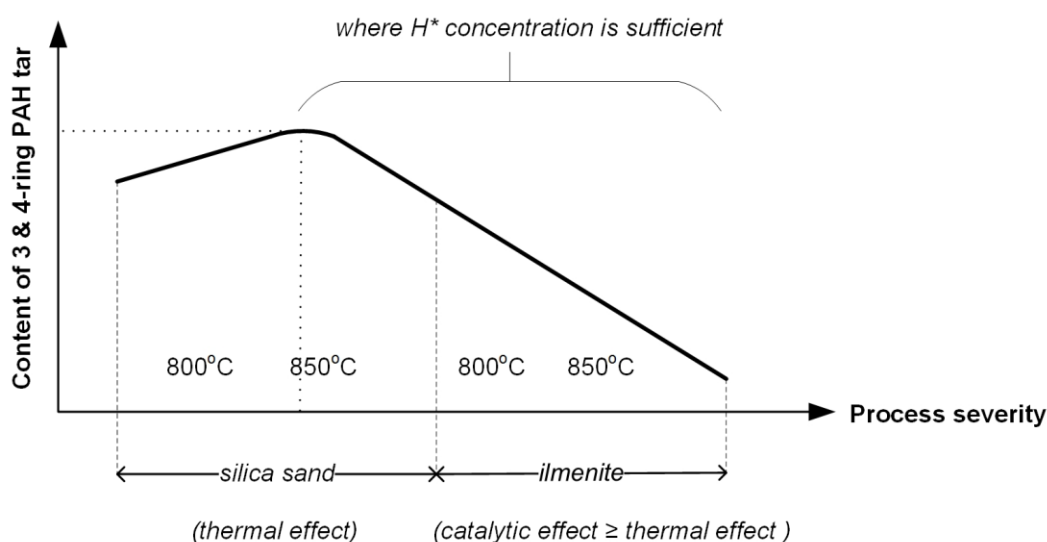


Figure 23. Illustration of the relationship between the content of 3 & 4-ring PAH tar (i.e., phenanthrene, anthracene, fluoranthene, pyrene, and chrysene) in the upgraded gas and the process severity.

The increased content of PAH tar in the upgraded gas indicates mutual combination of C^* . Since dibenzofuran and biphenyl are less stable than 3 & 4-ring compounds, the trend for C^* combines to produce 3 & 4-ring compounds is more prominent than the trend for C^* to combine to produce dibenzofuran and biphenyl at a higher process severity [71, 77]. This explains the shifting of these two compounds into 3 & 4-ring compounds in the silica sand experiments when the temperature was changed from 800°C to 850°C. Presumably, if steam and H_2 did not participate in the reactions, growth of PAH tar would always be increased following an increase in residence time in the silica sand experiments conducted at 850°C, as is also reported in the literature for a reaction environment in which steam and H_2 are deficient [10, 64, 66, 115, 116]. However, the obtained results show that the growth of PAH tar was increased to a certain level and then decreased. Thus, the more likely scenario is that the mutual combination of C^* is enhanced until the process severity is sufficiently high to induce a concentration of H^* that is capable of preventing the mutual combination of C^* . From this level of process severity and upwards, PAH growth is suppressed, whereby smaller products are produced.

Overall, the obtained results show that the principle of using steam and H_2 to limit the growth of PAH tar needs to be applied in combination with optimization of the process severity. To limit the growth of PAH tar, it is essential that the process severity is sufficiently high to convert steam and H_2 into reactive hydrogen intermediates that terminate the carbon-containing intermediates, thereby preventing combination of the carbon-containing intermediates. The results establish principles that can be used to reduce the growth of PAH tar during the tertiary conversion stage of biomass steam gasification conducted in, for example, dual fluidized bed gasifiers. When silica sand is used as the bed material, relatively high operating temperatures

and/or low-level steam fluidization in the gasifiers for long gas residence times are necessary. This could result in problems related to, e.g., bed agglomeration, or poor conversion of biomass due to a low steam-to-biomass ratio. If the catalytic bed is used to replace entirely the silica sand bed, an operating temperature lower than that required for the inert silica sand can be applied. The obtained results show that even the use of less-active materials, such as ilmenite, is an efficient solution.

6.4. General discussion and suggestions for future studies

6.4.1. General discussion

The results obtained from the conducted experiments reveal the essential roles of the interactions that occur between three types of reactive intermediates, i.e., C^* , H^* , and O^* , in determining the nature of the products formed during the raw gas upgrading. Thus, the principal features of the petrochemical processes discussed earlier have been applied successfully to explain the raw gas upgrading. For a given composition of the raw gas, the process severity is essential for modulating the concentrations of C^* , H^* and O^* in the reaction environment, and thereby the nature of the products formed. From the experimental observations, the product selectivity (Figure 5) is further clarified in relation to the process severity, as shown in Figure 24. If only the thermal effect is present, the tendency for mutual combination of C^* to form PAH tar is relatively strong. This tendency is suppressed as catalyst is used; the use of less-active catalysts, such as ilmenite, is an efficient solution. The level of H^* in the reaction environment is sufficient, such that relatively smaller and more stable tar/light HC (C_xH_y) are formed. Whether or not C_xH_y can be degraded in the same way as the parent tar/light HC depends on the process severity. An abundance of C_xH_y in the upgraded gas indicates that a higher level of process severity is necessary if C_xH_y is to be decomposed. The case in which all the tar and light HC are converted completely into CO/CO_2 requires the highest level of process severity.

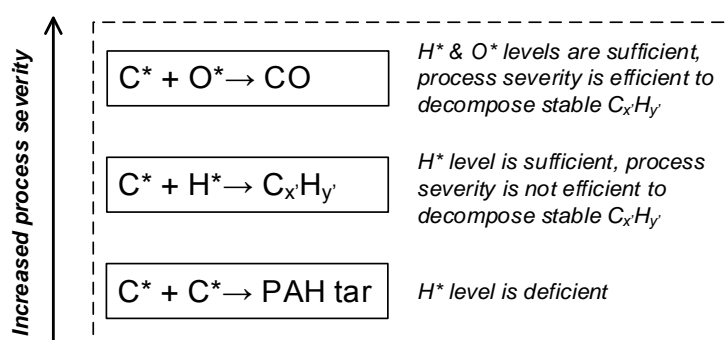


Figure 24. Relationships between product selectivity and process severity.

The proposed mechanism and, especially, the principle of product selectivity are implemented in developing the kinetic model for catalytic raw gas upgrading. The use of the raw gas produced in an industrial-scale gasifier and the fact that the applied measurements could detect all potential carbon-containing components, establish the reliability of the results obtained with the model. The introduction to the model of coefficients that represent product distribution (i.e., w_i and p_i) makes the model more informative in terms of the products formed during the upgrading process. The concept of formation and distribution of the pseudo-tar facilitates to handle the *in situ* formed tar and light HC, which is one of the main challenges in formulating the kinetic models. The pseudo-tar lumps together all the tar and light HC *in situ*, however, knowledge as to the extent to which the *in situ* formation of one tar group or light HC group is attributable to the destruction of the other tar and light HC groups can be acquired through further calculation (detailed data are shown in **Paper I**). From the results of the model calculation, a scheme that describes, in general terms, the gradual evolution of tar and light HC during the catalytic raw gas upgrading (Figure 25) is formulated.

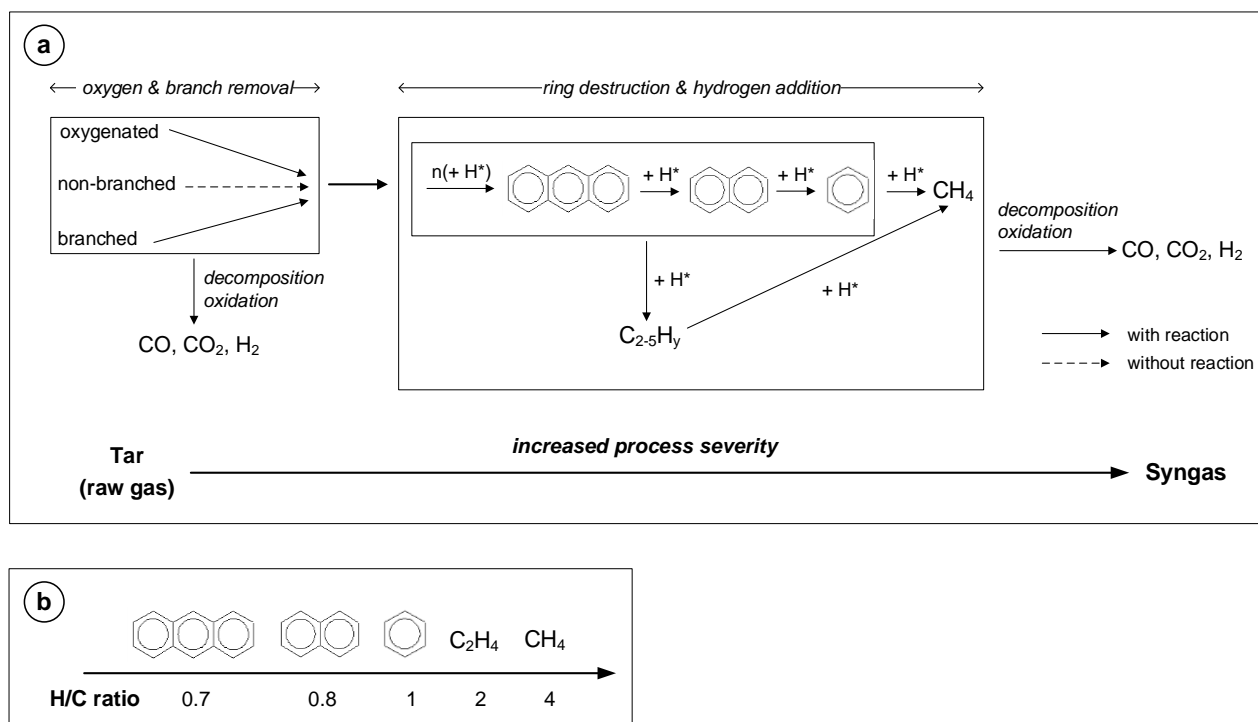


Figure 25, a–b. Evolution of tar and light HC during catalytic raw upgrading: **a)** Evolution scheme; **b)** H/C ratios of representative tar and light HC components involved in the evolution scheme.

In Figure 25, syngas is defined as the final product of the upgrading process, while the formation of relatively larger products is not considered. Initially, the oxygenated and branched aromatics are stripped of oxygen and branches, to produce non-branched aromatics that are more stable. In the next step, destruction of the aromatic ring occurs. The number of aromatic rings in the tar molecules gradually decreases, and ultimately, the tar in the upgraded gas

contains mostly benzene. In addition to CO, CO₂, and H₂ as permanent gases, CH₄ and other light HC (C₂₋₅H_y) are also produced during tar destruction. Furthermore, the destruction of C₂₋₅H_y can result in the formation of CH₄. As steam and H₂ are present in the reaction environment, the addition of hydrogen atoms to carbon-containing intermediates (which originate from tar and light HC) produces more-stable products, and eventually yields CH₄. Based on the scheme, the operating conditions for optimizing the formation of desired products can be determined. For example, ilmenite represents a good choice if benzene and CH₄ are the desired products from catalytic upgrading of the raw gas, as evidenced by the results obtained from the conducted experiments. However, if syngas is the expected product, uses of extensive gas-solid contact times or a higher operating temperature or catalysts with higher catalytic activity are necessary.

6.4.2. Suggestion for future studies

Although the model shows strong potential for describing and predicting the raw gas upgrading process, additional investigations are needed to refine the model, thereby improving further the description of the upgrading process. The following future studies are suggested:

- The validation of the calculated data of the model, and investigations regarding applications of the activation energies are needed, as discussed earlier;
- Additional tar components that are representative of the steps in the evolution scheme of tar and light HC should be investigated individually, as should mixtures thereof. This would provide a more comprehensive overview of the events that can take place during the authentic upgrading process. Based on that outcome, the criteria and the assumptions made for the selection of model coefficients could also be refined; and
- Application of the kinetic model for catalysts other than ilmenite is recommended. This is to investigate how the model can be adapted to other catalysts with their own specific activities. Thereby, other features of the upgrading process might be elucidated.

7. Conclusions and outlook

This work aimed to achieve a better understanding of the evolution of aromatic tar during the catalytic upgrading of a raw gas for tar removal. The emphasis was on a mature tar-containing raw gas produced in the Chalmers 2–4-MW_{th} dual fluidized bed biomass gasifier. Furthermore, as the raw gas upgrading comprises the different petrochemical processes, the principal chemistry of the most relevant petrochemical processes was taken as the basis for the work. To describe the gradual conversion of tar and light hydrocarbons during the raw gas upgrading process and the main trends of product formation, a reactive intermediate-based mechanism was formulated. The mechanism simplifies the process into interactions between three types of reactive intermediates, i.e., carbon-containing intermediates (C^{*}), hydrogen intermediates (H^{*}), and oxygen intermediates (O^{*}), in which C^{*} originate from tar and light hydrocarbons, and H^{*} and O^{*} originate most likely from the steam, H₂, and CO₂ in the raw gas. The interactions between C^{*} and O^{*}, and those between C^{*} and H^{*} produce smaller products, while the interactions of C^{*} with themselves contribute to the formation of larger products. The mechanism was further applied together with experimental data to elucidate the different features of the product selectivity inherent to the upgrading process. The experiments were conducted in laboratory-scale and bench-scale bubbling fluidized bed reactors. Ilmenite was used as the catalytic bed material, and inert silica sand was used for comparison. The gases fed to the reactors were the raw gas produced in the Chalmers gasifier and synthetic reactant gas mixtures that mimicked the composition of the Chalmers raw gas. From the obtained results, the following conclusions are drawn:

- Using the mechanism for the formation of relatively lighter products and the experimental results from using synthetic gas mixtures and ilmenite activated *in situ* during the course of the experiments, the contributions of the different decomposition reactions to the conversion of tar and light hydrocarbons are elucidated. For the given upgrading process, complete steam reforming, steam dealkylation, and hydro-cracking reactions are important, whereas the dry reforming reaction is not relevant;
- An eight-lump kinetic model that describes the catalytic raw gas upgrading is formulated based on the rate-determining steps assumed in the mechanism, and based on the distributions of CO/CO₂ and smaller tar/light hydrocarbons as the products from the destruction of the parent tar/light hydrocarbons. The results regarding the contributions of the different decomposition reactions were used as an input to the model. By fitting the model to the experimental data obtained from the upgrading of the Chalmers raw gas using a process-activated ilmenite catalyst from the Chalmers 12-MW_{th} boiler, the composition of the upgraded gas as a function of the gas-solid contact time is derived for different operating conditions. The evaluations of the applicability of the model confirm

that the model is capable of describing the process. Further studies are needed to clarify the potential of the formulated model; and

- Using the mechanism for the formation of relatively larger products and the experimental results for the upgrading process that was conducted using the Chalmers raw gas, with process-activated ilmenite and silica sand as bed materials, the fate of the PAH tar in relation to the process severity during the tertiary conversion stage of steam gasification of biomass was revealed. It is confirmed that utilizing the steam and H_2 available in the reaction environment can reduce the growth of PAH tar. The process severity needs to be sufficient to convert steam and H_2 into the hydrogen intermediates H^* that terminate C^* , such that the mutual combinations of C^* are prevented. To ensure this within the temperature range of 800–850°C, which is relevant for operation of the fluidized bed gasifier, the catalytic effect of less-active materials, such as ilmenite, is adequate.

This work proves the principles that determine the nature of the products formed during the raw gas upgrading, as well as the relationship between the process severity and the nature of the products. The obtained results, on the one hand, provide a basis for optimization and upscaling of the catalytic raw gas upgrading process. On the other hand, they represent an essential input for the development of comprehensive models, in that the complicated features of the upgrading process are incorporated fully rather than the features being simplified. In particular, for the detailed kinetic models currently available in the literature, the obtained results provide insights into the criteria for the selection of elementary reactions that are practically relevant. In this way, the detailed kinetic models describe comprehensively the upgrading process and highlight the potential for practical applications. Finally, the results of this work confirm the similarity between raw gas upgrading and petrochemical processes. Thus, the mature knowledge of the petroleum refinery should be investigated further in terms of application to the gasification context.

References

- [1] E4Tech, *Review of Technologies for Gasification of Biomass and Wastes*, 2009, National Non-Food Crops Centre: United Kingdom.
- [2] Bridgwater, A. V., *Renewable fuels and chemicals by thermal processing of biomass*. Chemical Engineering Journal, 2003. **91**: p. 87–102.
- [3] Sikarwar, V. S.; Zhao, M.; Clough, P.; Yao, J.; Zhong, X.; Memon, M. Z.; Shah, N.; Anthony, E. J.; Fennell, P. S., *An overview of advances in biomass gasification*. Energy & Environmental Science, 2016. **9**: p. 2939–2977.
- [4] Claude, V.; Courson, C.; Köhler, M.; Lambert, S. D., *Overview and Essentials of Biomass Gasification Technologies and Their Catalytic Cleaning Methods*. Energy & Fuels, 2016. **30**: p. 8791–8814.
- [5] Larsson, A.; Seemann, M.; Neves, D.; Thunman, H., *Evaluation of Performance of Industrial-Scale Dual Fluidized Bed Gasifiers Using the Chalmers 2–4-MWth Gasifier*. Energy & Fuels, 2013. **27**: p. 6665–6680.
- [6] Milne, T. A.; Evans, R. J.; Abatzoglou, N., *Biomass Gasifier “Tars”: Their Nature, Formation, and Conversion*, 1998, National Renewable Energy Laboratory: Golden, Colorado.
- [7] Li, C.; Suzuki, K., *Tar property, analysis, reforming mechanism and model for biomass gasification-An overview*. Renewable & Sustainable Energy Reviews, 2009. **13**: p. 594–604.
- [8] Torres, W.; Pansare, S. S.; Goodwin, J. G., *Hot Gas Removal of Tars, Ammonia, and Hydrogen Sulfide from Biomass Gasification Gas*. Catalysis Reviews-Science and Engineering, 2007. **49**: p. 407–456.
- [9] Devi, L.; Ptasinski, K. J.; Janssen, F. J. J. G., *A review of the primary measures for tar elimination in biomass gasification processes*. Biomass & Bioenergy, 2003. **24**: p. 125–140.
- [10] Evans, R. J.; Milne, T. A., *Chemistry of Tar Formation and Maturation in the Thermochemical Conversion of Biomass*, in *Developments in Thermochemical Biomass Conversion: Volume 1/Volume 2*, A.V. Bridgwater and D.G.B. Boocock, Editors. 1997, Springer Netherlands: Dordrecht. p. 803–816.
- [11] Larsson, A.; Israelsson, M.; Lind, F.; Seemann, M.; Thunman, H., *Using Ilmenite To Reduce the Tar Yield in a Dual Fluidized Bed Gasification System*. Energy & Fuels, 2014. **28**: p. 2632–2644.
- [12] Marinkovic, J.; Thunman, H.; Knutsson, P.; Seemann, M., *Characteristics of olivine as a bed material in an indirect biomass gasifier*. Chemical Engineering Journal, 2015. **279**: p. 555–566.

- [13] Berdugo Vilches, T.; Marinkovic, J.; Seemann, M.; Thunman, H., *Comparing Active Bed Materials in a Dual Fluidized Bed Biomass Gasifier: Olivine, Bauxite, Quartz-Sand, and Ilmenite*. *Energy & Fuels*, 2016. **30**: p. 4848–4857.
- [14] Basu, P., *Chapter 4 - Tar Production and Destruction*, in *Biomass Gasification and Pyrolysis* 2010, Academic Press: Boston. p. 97–116.
- [15] Anis, S.; Zainal, Z. A., *Tar reduction in biomass producer gas via mechanical, catalytic and thermal methods: A review*. *Renewable and Sustainable Energy Reviews*, 2011. **15**: p. 2355–2377.
- [16] Boerrigter, H.; van Paasen, S. V. B.; Bergman, P. C. A.; Könemann, J. W.; Emmen, R.; Wijnands, A., *“OLGA” TAR REMOVAL TECHNOLOGY: Proof-of-Concept (PoC) for application in integrated biomass gasification combined heat and power (CHP) systems*, 2005, Energy Research Centre of the Netherlands.
- [17] Zwart, R. W. R.; Boerrigter, H.; Deurwaarder, E. P.; van der Meijden, C. M.; van Paasen, S. V. B., *Production of Synthetic Natural Gas (SNG) from Biomass*, 2006, Energy Research Centre of the Netherlands.
- [18] Abdoulmoumine, N.; Adhikari, S.; Kulkarni, A.; Chattanathan, S., *A review on biomass gasification syngas cleanup*. *Applied Energy*, 2015. **155**: p. 294–307.
- [19] Woolcock, P. J.; Brown, R. C., *A review of cleaning technologies for biomass-derived syngas*. *Biomass and Bioenergy*, 2013. **52**: p. 54–84.
- [20] Larsson, A., *Fuel conversion in a dual fluidized bed gasifier - Experimental quantification and impact on performance*, 2014, Chalmers University of Technology: Gothenburg, Sweden.
- [21] Singh, R. N.; Singh, S. P.; Balwanshi, J. B., *Tar removal from Producer Gas: A Review*. *Research Journal of Engineering Sciences*, 2014. **3**: p. 16–22.
- [22] Speight, J. G., *Chapter 16 - Hydroprocessing*, in *The Chemistry and Technology of Petroleum* 1999, CRC Press: New York. p. 604–640.
- [23] Fahim, M. A.; Alsahhaf, T. A.; Elkilani, A., *Chapter 11 - Hydrogen Production*, in *Fundamentals of Petroleum Refining* 2010, Elsevier: Amsterdam. p. 153–198.
- [24] Fahim, M. A.; Alsahhaf, T. A.; Elkilani, A., *Chapter 7 - Hydroconversion*, in *Fundamentals of Petroleum Refining* 2010, Elsevier: Amsterdam. p. 153–198.
- [25] Fahim, M. A.; Alsahhaf, T. A.; Elkilani, A., *Chapter 6 - Thermal Cracking and Coking*, in *Fundamentals of Petroleum Refining* 2010, Elsevier: Amsterdam. p. 123–152.
- [26] Fahim, M. A.; Alsahhaf, T. A.; Elkilani, A., *Chapter 8 - Fluidised catalytic cracking*, in *Fundamentals of Petroleum Refining* 2010, Elsevier: Amsterdam. p. 153–198.

- [27] Speight, J. G., *Chapter 11 - Thermal Decomposition of Hydrocarbons*, in *Handbook of Industrial Hydrocarbon Processes* 2011, Gulf Professional Publishing: Boston. p. 395–428.
- [28] Fahim, M. A.; Alsahhaf, T. A.; Elkilani, A., *Chapter 2 - Refinery Feedstocks and Products*, in *Fundamentals of Petroleum Refining* 2010, Elsevier: Amsterdam. p. 11–31.
- [29] Speight, J. G., *Chapter 12 - Refining Chemistry*, in *The Chemistry and Technology of Petroleum* 1999, CRC Press: New York. p. 499–535.
- [30] Speight, J. G., *Chapter 14 - Thermal Cracking*, in *The Chemistry and Technology of Petroleum* 1999, CRC Press: New York. p. 565–584.
- [31] Speight, J. G., *Chapter 22 - Hydrogen Production*, in *The Chemistry and Technology of Petroleum* 2007, CRC Press: New York. p. 637–660.
- [32] Srinivas, S.; Field, R. P.; Herzog, H. J., *Modeling Tar Handling Options in Biomass Gasification*. *Energy & Fuels*, 2013. **27**: p. 2859–2873.
- [33] Jönsson, O., *Thermal Cracking of Tars and Hydrocarbons by Addition of Steam and Oxygen in the Cracking Zone*, in *Fundamentals of Thermochemical Biomass Conversion* 1985. p. 733–746.
- [34] Houben, M. P.; de Lange, H. C.; van Steenhoven, A. A., *Tar reduction through partial combustion of fuel gas*. *Fuel*, 2005. **84**: p. 817–824.
- [35] Lind, F.; Seemann, M.; Thunman, H., *Continuous Catalytic Tar Reforming of Biomass Derived Raw Gas with Simultaneous Catalyst Regeneration*. *Industrial & Engineering Chemistry Research*, 2011. **50**: p. 11553–11562.
- [36] Lind, F., *Design and Operation of a Chemical-Looping Reformer for Catalytic Upgrading of Biomass-Derived Gas*, 2013, Chalmers University of Technology: Gothenburg, Sweden.
- [37] Yung, M. M.; Jablonski, W. S.; Magrini-Bair, K. A., *Review of catalytic conditioning of biomass-derived syngas*. *Energy & Fuels*, 2009. **23**: p. 1874–1887.
- [38] Rönkkönen, H.; Simell, P.; Reinikainen, M.; Krause, O.; Niemelä, M. V., *Catalytic clean-up of gasification gas with precious metal catalysts – A novel catalytic reformer development*. *Fuel*, 2010. **89**: p. 3272–3277.
- [39] Dayton, D., *A Review of the Literature on Catalytic Biomass Tar Destruction* 2002, National Renewable Energy Laboratory: Golden, Colorado.
- [40] Shen, Y.; Yoshikawa, K., *Recent progresses in catalytic tar elimination during biomass gasification or pyrolysis-A review*. *Renewable and Sustainable Energy Reviews*, 2013. **21**: p. 371–392.
- [41] Chan, F. L.; Tanksale, A., *Review of recent developments in Ni-based catalysts for biomass gasification*. *Renewable and Sustainable Energy Reviews*, 2014. **38**: p. 428–438.

- [42] Delgado, J.; Aznar, M. P.; Corella, J., *Calcined Dolomite, Magnesite, and Calcite for Cleaning Hot Gas from a Fluidized Bed Biomass Gasifier with Steam: Life and Usefulness*. Industrial & Engineering Chemistry Research, 1996. **35**: p. 3637–3643.
- [43] Lind, F.; Berguerand, N.; Seemann, M.; Thunman, H., *Ilmenite and Nickel as Catalysts for Upgrading of Raw Gas Derived from Biomass Gasification*. Energy & Fuels, 2013. **27**: p. 997–1007.
- [44] Lind, F.; Israelsson, M.; Seemann, M.; Thunman, H., *Manganese oxide as catalyst for tar cleaning of biomass-derived gas*. Biomass Conversion and Biorefinery, 2012. **2**: p. 133–140.
- [45] Thunman, H.; Berguerand, N.; Seemann, M., *Advanced Gas Cleaning using Chemical-Looping Reforming (CLR)*, in *1st International Conference on Renewable Energy Gas Technology 2014*: Malmö, Sweden.
- [46] Świerczyński, D.; Libs, S.; Courson, C.; Kiennemann, A., *Steam reforming of tar from a biomass gasification process over Ni/olivine catalyst using toluene as a model compound*. Applied Catalysis B, 2007. **74**: p. 211–222.
- [47] Devi, L.; Ptasinski, K. J.; Janssen, F. J. J. G., *Pretreated olivine as tar removal catalyst for biomass gasifiers: investigation using naphthalene as model biomass tar*. Fuel Processing Technology, 2005. **86**: p. 707–730.
- [48] Jess, A., *Mechanisms and kinetics of thermal reactions of aromatic hydrocarbons from pyrolysis of solid fuels*. Fuel, 1996. **75**: p. 1441–1448.
- [49] Simell, P. A.; Hirvensalo, E. K.; Smolander, V. T.; Krause, A. O. I., *Steam Reforming of Gasification Gas Tar over Dolomite with Benzene as a Model Compound*. Industrial & Engineering Chemistry Research, 1999. **38**: p. 1250–1257.
- [50] Aldén, H.; Björkman, E.; Carlsson, M.; Waldheim, L., *Catalytic Cracking of Naphthalene on Dolomite*, in *Advances in Thermochemical Biomass Conversion*, A.V. Bridgwater, Editor 1993, Springer Netherlands. p. 216–232.
- [51] Tamhankar, S. S.; Tsuchiya, K.; Riggs, J. B., *Catalytic cracking of benzene on iron oxide-silica: catalyst activity and reaction mechanism*. Applied Catalysis, 1985. **16**: p. 103–121.
- [52] Corella, J.; Narváez, I.; Orío, A. *Criteria for selection of dolomites and catalysts for tar elimination from gasification gas; kinetic constants*. in *VTT Symposium 163*. 1996, Finland.
- [53] Corella, J.; Toledo, J. M.; Aznar, M.-P., *Improving the Modeling of the Kinetics of the Catalytic Tar Elimination in Biomass Gasification*. Industrial & Engineering Chemistry Research, 2002. **41**: p. 3351–3356.

- [54] Corella, J.; Caballero, M. A.; Aznar, M.-P.; Brage, C., *Two Advanced Models for the Kinetics of the Variation of the Tar Composition in Its Catalytic Elimination in Biomass Gasification*. *Industrial & Engineering Chemistry Research*, 2003. **42**: p. 3001–3011.
- [55] Fuentes-Cano, D.; Gómez-Barea, A.; Nilsson, S.; Ollero, P., *Kinetic Modeling of Tar and Light Hydrocarbons during the Thermal Conversion of Biomass*. *Energy & Fuels*, 2016. **30**: p. 377–385.
- [56] Israelsson, M.; Thunman, H., *Gasification Reaction Pathways of Condensable Hydrocarbons*. *Energy & Fuels*, 2016. **30**: p. 4951–4959.
- [57] Font Palma, C., *Model for Biomass Gasification Including Tar Formation and Evolution*. *Energy & Fuels*, 2013. **27**: p. 2693–2702.
- [58] Norinaga, K.; Sakurai, Y.; Sato, R.; Hayashi, J.-i., *Numerical simulation of thermal conversion of aromatic hydrocarbons in the presence of hydrogen and steam using a detailed chemical kinetic model*. *Chemical Engineering Journal*, 2011. **178**: p. 282–290.
- [59] Debiagi, P. E. A.; Gentile, G.; Pelucchi, M.; Frassoldati, A.; Cuoci, A.; Faravelli, T.; Ranzi, E., *Detailed kinetic mechanism of gas-phase reactions of volatiles released from biomass pyrolysis*. *Biomass and Bioenergy*, 2016. **93**: p. 60–71.
- [60] Min, Z.; Asadullah, M.; Yimsiri, P.; Zhang, S.; Wu, H.; Li, C.-Z., *Catalytic reforming of tar during gasification. Part I. Steam reforming of biomass tar using ilmenite as a catalyst*. *Fuel*, 2011. **90**: p. 1847–1854.
- [61] Keller, M.; Leion, H.; Mattisson, T.; Thunman, H., *Investigation of Natural and Synthetic Bed Materials for Their Utilization in Chemical Looping Reforming for Tar Elimination in Biomass-Derived Gasification Gas*. *Energy & Fuels*, 2014. **28**: p. 3833–3840.
- [62] Evans, R. J.; Milne, T. A., *Molecular characterization of the pyrolysis of biomass. 1. Fundamentals*. *Energy & Fuels*, 1987. **1**: p. 123–137.
- [63] Morf, P.; Hasler, P.; Nussbaumer, T., *Mechanisms and kinetics of homogeneous secondary reactions of tar from continuous pyrolysis of wood chips*. *Fuel*, 2002. **81**: p. 843–853.
- [64] Kinoshita, C. M.; Wang, Y.; Zhou, J., *Tar formation under different biomass gasification conditions*. *Journal of Analytical and Applied Pyrolysis*, 1994. **29**: p. 169–181.
- [65] Israelsson, M.; Berdugo Vilches, T.; Thunman, H., *Conversion of Condensable Hydrocarbons in a Dual Fluidized Bed Biomass Gasifier*. *Energy & Fuels*, 2015. **29**: p. 6465–6475.
- [66] Stiles, H. N.; Kandiyoti, R., *Secondary reactions of flash pyrolysis tars measured in a fluidized bed pyrolysis reactor with some novel design features*. *Fuel*, 1989. **68**: p. 275–282.

- [67] Churin, E.; Maggi, R.; Grange, P.; Delmon, B., *Characterization and Upgrading of a Bio-Oil Produced by Pyrolysis of Biomass*, in *Research in Thermochemical Biomass Conversion*, A.V. Bridgwater and J.L. Kuester, Editors. 1988, Springer Netherlands: Dordrecht. p. 896–909.
- [68] Essig, M.; Lowary, T.; Richards, G. N.; Schenck, E., *Influences of “Neutral” Salts on Thermochemical Conversion of Cellulose and of Sucrose*, in *Research in Thermochemical Biomass Conversion*, A.V. Bridgwater and J.L. Kuester, Editors. 1988, Springer Netherlands: Dordrecht. p. 143–154.
- [69] Ledesma, E. B.; Marsh, N. D.; Sandrowitz, A. K.; Wornat, M. J., *An experimental study on the thermal decomposition of catechol*. Proceedings of the Combustion Institute, 2002. **29**: p. 2299–2306.
- [70] Cypres, R., *Aromatic hydrocarbons formation during coal pyrolysis*. Fuel Processing Technology, 1987. **15**: p. 1–15.
- [71] Bruinsma, O. S. L.; Moulijn, J. A., *The pyrolytic formation of polycyclic aromatic hydrocarbons from benzene, toluene, ethylbenzene, styrene, phenylacetylene and n-decane in relation to fossil fuels utilization*. Fuel Processing Technology, 1988. **18**: p. 213–236.
- [72] Zanetti, J. E.; Egloff, G., *The Thermal Decomposition of Benzene*. Journal of Industrial & Engineering Chemistry, 1917. **9**: p. 350–356.
- [73] Badger, G. M.; Novotny, J., *661. The formation of aromatic hydrocarbons at high temperatures. Part XII. The pyrolysis of benzene*. Journal of the Chemical Society (Resumed), 1961: p. 3400–3402.
- [74] Scheer, A. M.; Mukarakate, C.; Robichaud, D. J.; Ellison, G. B.; Nimlos, M. R., *Radical Chemistry in the Thermal Decomposition of Anisole and Deuterated Anisoles: An Investigation of Aromatic Growth*. The Journal of Physical Chemistry A, 2010. **114**: p. 9043–9056.
- [75] Gräber, W.-D.; Hüttinger, K. J., *Chemistry of methane formation in hydrogasification of aromatics. 1. Non-substituted aromatics*. Fuel, 1982. **61**: p. 499–504.
- [76] Gräber, W.-D.; Hüttinger, K. J., *Chemistry of methane formation in hydrogasification of aromatics. 3. Aromatics with heteroatoms*. Fuel, 1982. **61**: p. 510–515.
- [77] Fuentes-Cano, D.; Gómez-Barea, A.; Nilsson, S.; Ollero, P., *The influence of temperature and steam on the yields of tar and light hydrocarbon compounds during devolatilization of dried sewage sludge in a fluidized bed*. Fuel, 2013. **108**: p. 341–350.
- [78] Vreugdenhil, B. J.; Zwart, R. W. R., *Tar formation in pyrolysis and gasification*, 2009, Energy Research Centre of the Netherlands.

- [79] Debiagi, P. E. A.; Pecchi, C.; Gentile, G.; Frassoldati, A.; Cuoci, A.; Faravelli, T.; Ranzi, E., *Extractives Extend the Applicability of Multistep Kinetic Scheme of Biomass Pyrolysis*. *Energy & Fuels*, 2015. **29**: p. 6544–6555.
- [80] Simell, P. A.; Hepola, J. O.; Krause, A. O. I., *Effects of gasification gas components on tar and ammonia decomposition over hot gas cleanup catalysts*. *Fuel*, 1997. **76**: p. 1117–1127.
- [81] Ratnasamy, C.; Wagner, J. P., *Water Gas Shift Catalysis*. *Catalysis Reviews*, 2009. **51**: p. 325–440.
- [82] Rostrup-Nielsen, J. R., *Catalytic Steam Reforming*, in *Catalysis*, J.R. Anderson and M. Boudart, Editors. 1984, Springer Berlin Heidelberg. p. 1–117.
- [83] de Klerk, A., *Cracking, in Fischer-Tropsch Refining* 2011, Wiley. p. 407–440.
- [84] Duprez, D., *Selective steam reforming of aromatic compounds on metal catalysts*. *Applied Catalysis A*, 1992. **82**: p. 111–157.
- [85] Blanksby, S. J.; Ellison, G. B., *Bond Dissociation Energies of Organic Molecules*. *Accounts of Chemical Research*, 2003. **36**: p. 255–263.
- [86] Dean, J. A., *Properties of atoms, radicals, and bonds*, in *Lange's handbook of chemistry* 1999, McGraw-Hill.
- [87] Carey, F. A.; Sundberg, R. J., *Advanced Organic Chemistry. Part A: Structure and Mechanisms* 2007, New York: Springer.
- [88] Ouellette, R. J.; Rawn, J. D., *Chapter 12 - Arenes and Aromaticity*, in *Organic Chemistry* 2014, Elsevier: Boston. p. 397–415.
- [89] Sarioğlan, A., *Tar removal on dolomite and steam reforming catalyst: Benzene, toluene and xylene reforming*. *International Journal of Hydrogen Energy*, 2012. **37**: p. 8133–8142.
- [90] Wittcoff, H. A.; Reuben, B. G.; Plotkin, J. S., *Chapter 4 - Chemicals from Natural Gas and Petroleum*, in *Industrial Organic Chemicals* 2012, John Wiley & Sons, Inc. p. 93–138.
- [91] Taralas, G., *Modeling the influence of mineral rocks, active in different hot gas conditioning systems and technologies, on the production of light α -olefins*. *Canadian Journal of Chemical Engineering*, 1999. **77**: p. 1205–1214.
- [92] Taralas, G.; Kontominas, M. G.; Kakatsios, X., *Modeling the Thermal Destruction of Toluene (C_7H_8) as Tar-Related Species for Fuel Gas Cleanup*. *Energy & Fuels*, 2003. **17**: p. 329–337.
- [93] Robaugh, D.; Tsang, W., *Mechanism and rate of hydrogen atom attack on toluene at high temperatures*. *Journal of Physical Chemistry*, 1986. **90**: p. 4159–4163.

- [94] Shah, Y. T.; Gardner, T. H., *Dry Reforming of Hydrocarbon Feedstocks*. Catalysis Reviews, 2014. **56**: p. 476–536.
- [95] Wei, J.; Iglesia, E., *Isotopic and kinetic assessment of the mechanism of methane reforming and decomposition reactions on supported iridium catalysts*. Physical Chemistry Chemical Physics, 2004. **6**: p. 3754–3759.
- [96] Murzin, D.; Salmi, T., *Heterogeneous catalytic kinetics*, in *Catalytic Kinetics 2005*, Elsevier Science: Amsterdam. p. 225–284.
- [97] Golombok, M., *Steam Hydrocarbon Cracking and Reforming*. Journal of Chemical Education, 2004. **81**: p. 228.
- [98] Henderson, M. A., *The interaction of water with solid surfaces: fundamental aspects revisited*. Surface Science Report, 2002. **46**: p. 1–308.
- [99] Thunman, H.; Lind, F.; Breitholtz, C.; Berguerand, N.; Seemann, M., *Using an oxygen-carrier as bed material for combustion of biomass in a 12-MWth circulating fluidized-bed boiler*. Fuel, 2013. **113**: p. 300–309.
- [100] Israelsson, M.; Seemann, M.; Thunman, H., *Assessment of the Solid-Phase Adsorption Method for Sampling Biomass-Derived Tar in Industrial Environments*. Energy & Fuels, 2013. **27**: p. 7569–7578.
- [101] Leion, H.; Lyngfelt, A.; Johansson, M.; Jerndal, E.; Mattisson, T., *The use of ilmenite as an oxygen carrier in chemical-looping combustion*. Chemical Engineering Research and Design, 2008. **86**: p. 1017–1026.
- [102] Adánez, J.; Cuadrat, A.; Abad, A.; Gayán, P.; Diego, L. F. D.; García-Labiano, F., *Ilmenite activation during consecutive redox cycles in chemical-looping combustion*. Energy & Fuels, 2010. **24**: p. 1402–1413.
- [103] Schwebel, G. L.; Leion, H.; Krumm, W., *Comparison of natural ilmenites as oxygen carriers in chemical-looping combustion and influence of water gas shift reaction on gas composition*. Chemical Engineering Research and Design, 2012. **90**: p. 1351–1360.
- [104] Corcoran, A.; Marinkovic, J.; Lind, F.; Thunman, H.; Knutsson, P.; Seemann, M., *Ash Properties of Ilmenite Used as Bed Material for Combustion of Biomass in a Circulating Fluidized Bed Boiler*. Energy & Fuels, 2014. **28**: p. 7672–7679.
- [105] Marinkovic, J.; Seemann, M.; Schwebel, G. L.; Thunman, H., *Impact of Biomass Ash–Bauxite Bed Interactions on an Indirect Biomass Gasifier*. Energy & Fuels, 2016. **30**: p. 4044–4052.
- [106] Kunii, D.; Levenspiel, O., *Chapter 3 - Fluidization and mapping of regimes*, in *Fluidization engineering* 1991, Butterworth - Heinemann.

- [107] Bruinsma, O. S. L.; Geertsma, R. S.; Bank, P.; Moulijn, J. A., *Gas phase pyrolysis of coal-related aromatic compounds in a coiled tube flow reactor: 1. Benzene and derivatives*. Fuel, 1988. **67**: p. 327–333.
- [108] Boroson, M. L.; Howard, J. B.; Longwell, J. P.; Peters, W. A., *Product yields and kinetics from the vapor phase cracking of wood pyrolysis tars*. AIChE Journal, 1989. **35**: p. 120–128.
- [109] Delgado, J.; Aznar, M. P.; Corella, J., *Biomass Gasification with Steam in Fluidized Bed: Effectiveness of CaO, MgO, and CaO–MgO for Hot Raw Gas Cleaning*. Industrial & Engineering Chemistry Research, 1997. **36**: p. 1535–1543.
- [110] Aznar, M. P.; Caballero, M. A.; Gil, J.; Martín, J. A.; Corella, J., *Commercial Steam Reforming Catalysts To Improve Biomass Gasification with Steam–Oxygen Mixtures. 2. Catalytic Tar Removal*. Industrial & Engineering Chemistry Research, 1998. **37**: p. 2668–2680.
- [111] Fuentes-Cano, D.; Gómez-Barea, A.; Nilsson, S.; Ollero, P., *Decomposition kinetics of model tar compounds over chars with different internal structure to model hot tar removal in biomass gasification*. Chemical Engineering Journal, 2013. **228**: p. 1223–1233.
- [112] Swierczynski, D.; Courson, C.; Kiennemann, A., *Study of steam reforming of toluene used as model compound of tar produced by biomass gasification*. Chemical Engineering and Processing: Process Intensification, 2008. **47**: p. 508–513.
- [113] Tinaut, F. V.; Melgar, A.; Pérez, J. F.; Horrillo, A., *Effect of biomass particle size and air superficial velocity on the gasification process in a downdraft fixed bed gasifier. An experimental and modelling study*. Fuel Processing Technology, 2008. **89**: p. 1076–1089.
- [114] Rothenberg, G., *The Basics of Catalysis*, in *Catalysis 2008*, Wiley-VCH Verlag GmbH & Co. KGaA. p. 39–75.
- [115] Hayashi, J.; Nakagawa, K.; Kusakabe, K.; Morooka, S.; Yumura, M., *Change in molecular structure of flash pyrolysis tar by secondary reaction in a fluidized bed reactor*. Fuel Processing Technology, 1992. **30**: p. 237–248.
- [116] van Paasen, S. V. B.; Kiel, J. H. A., *Tar formation in a fluidised-bed gasifiers: Impact of fuel properties and operating conditions*, 2004, Energy Research Centre of the Netherlands.